

Figure 1. Flow cytometric analysis of hES-derived and iPS-derived cells on day 10 of differentiation. A through C, hES-derived cells (A, H9; B, HES3; C, KhES-1). D through G, iPS-derived cells (D, B6; E, B7; F, G1; G, G4). H and I, Analysis of human iPS-derived cells with other EC markers.

Results

We investigated 3 hES cell lines (H9, HES3, and KhES1) and 4 iPS cell lines (201B6, 201B7, 253G1, and 253G4).^{5,6} 201B6 (B6) and 201B7 (B7) cells were generated from human skin fibroblasts by transfection with 4 transcription factors (Oct3/4, Sox2, Klf4, c-Myc), whereas 253G1 (G1) and 253G4 (G4) were generated using only 3 factors (c-Myc was omitted).¹⁰ The morphology of these 4 lines did not differ from hES cells, and they were also positive for hES cell markers (supplemental Figure I). We induced differentiation of these iPS cell lines in an *in vitro* 2D culture system previously established for differentiation of hES cells into vascular cells.³ After 10 days of differentiation, cells positive for Flk1 (also designated VEGF receptor-2) and the EC marker VE-cadherin emerged and accounted for 1% to 5% of

the cells (Figure 1A through 1G). We noted no differences in the differentiation of the B and G lines, and both were comparable to the hES lines (Figure 1A through 1G). The Flk1⁺ VE-cadherin⁺ cell population was also positive for CD31 and CD34 (Figure 1H and 1I), and negative for the ES cell marker tumor rejection antigen 1–60 (TRA1–60). We sorted those cells and recultured with VEGF, and found that they formed a network-like structure on Matrigel, *in vitro* (Figure 2A), and had a cobblestone appearance when confluent on collagen IV-coated dishes (Figure 2B). Immunofluorescent staining for CD31 produced a characteristic marginal staining pattern (Figure 2C), and staining for endothelial NO synthase produced a cytoplasmic pattern (Figure 2D). Based on these observations, the cells were consistent with ECs. Subsequent RT-PCR analysis of EC markers revealed that both human iPS-derived and hES-derived ECs expressed

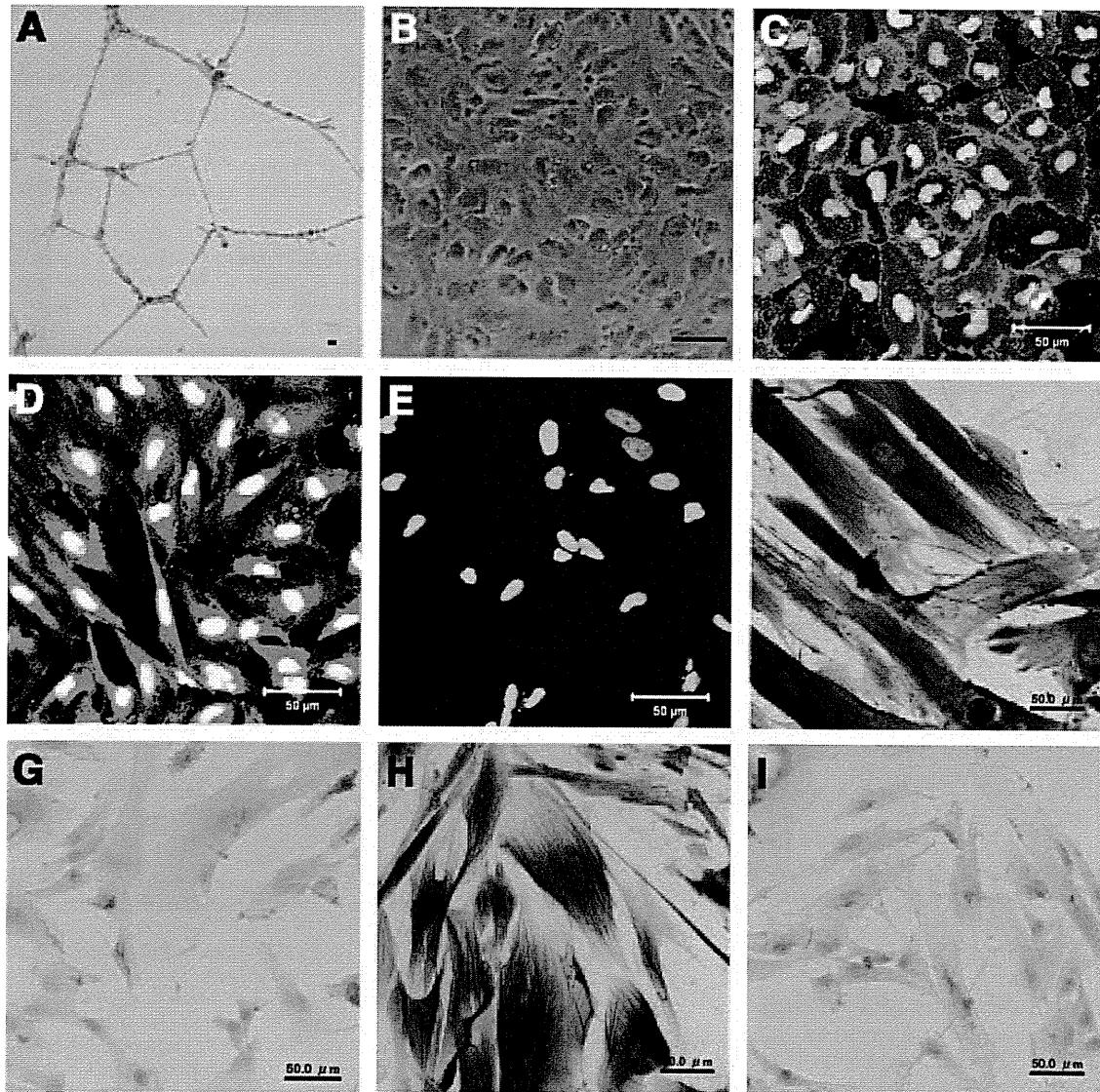


Figure 2. A, Network formation by iPS-derived VE-cadherin⁺ cells after 24 hours of culture on Matrigel. B, Phase-contrast photomicrograph of iPS-derived VE-cadherin⁺ cells. C through E, Immunostaining of VE-cadherin⁺ cells: red, CD31 (C) or eNOS (D) or control mouse IgG1 (E; as negative control for C and D); green, nuclei. F through I, Immunostaining of VE-cadherin⁻ Flk1⁺ cells for MC markers: F, α SMA; G, control mouse IgG2 (negative control for F); H, calponin; I, control mouse IgG1 κ (negative control for H). Scale bars=50 μ m.

VE-cadherin, CD31, von Willebrand factor (vWF), and CD34 at levels similar to those seen in adult ECs (supplemental Figure II).

We next sorted for Flk1⁺ VE-cadherin⁻ TRA1-60⁻ cells on day 10 of differentiation and then induced differentiation into MCs using PDGF-BB as described previously.^{3,4} Once differentiated, these cells stained positively for α SMA and calponin and were therefore consistent with MCs (Figure 2E and 2F). Both human iPS-derived and hES-derived MCs expressed the vascular smooth cell markers at levels similar to those seen in adult vascular smooth muscle cells (supplemental Figure II).

Discussion

The establishment of iPS cells opened a new avenue for regenerative medicine and stem cell biology. The directional

differentiation of mouse iPS cells into vascular cells was recently reported.¹¹ In the present study, we have shown that human iPS cells can be directionally differentiated into vascular ECs and MCs by applying the same methods we established for hES cells.³ We previously reported that the differentiation kinetics of primate ES cells to vascular cells is not equal to that of mouse ES cells.^{2,3} To further clarify the differentiation process in human beings and to determine the possible clinical application of iPS cells, investigation of human iPS cells is essential because some characters were significantly different between mouse and human iPS cells as ES cells.

In contrast to human ES cells, iPS cells can be established from every human being irrespective of their genetic backgrounds. The establishment of in vitro differentiation system of human vascular cells from human iPS cells should make it possible to dissect out cellular mechanisms

in human vascular development and diseased states such as arteriosclerosis. The establishment of iPS cell lines from patients with inherited diseases presenting vascular abnormality should enable clarification of their pathogenesis. In addition, because they overcome the immunologic and ethical problems associated with human ES cells, our study should also contribute to the development of novel patient-specific cell based vascular regenerative therapies.

Several issues remain to be resolved before human iPS-derived vascular cells can be administered to humans, however. Although we observed no reappearance of undifferentiated or tumor cell-like structures in the in vitro cultures, when we examined the mRNA expression of the transgenes during differentiation experiments, we occasionally observed upregulation of the transgenic mRNA (supplemental Figure III). The safety of iPS cells needs to be confirmed for each iPS cell line, both in vitro and in vivo.

In conclusion, we succeeded in inducing and isolating human vascular cells from iPS cells and indicate that the properties of differentiation are nearly identical to those of hES cells. This work will contribute to our understanding of human vascular differentiation/development and to the development of vascular regenerative medicine.

We described additional discussions about the safety of iPS cells in the supplemental material.

Acknowledgments

We thank Yoshie Fukuchi for her technical assistance. The anti-human Flk1 antibody (KM1668) was a generous gift from Kyowa Hakko Co Ltd.

Sources of Funding

This work was supported by the project for realization of regenerative medicine of the Ministry of Education, Culture, Sports, Science, and Technology, Japan, Grants-in-Aid for Scientific Research from the Ministry of Health, Labor, and Welfare, the Ministry of Education, Culture, Sports, Science, and Technology, the Takeda Science Foundation, the Japan Cardiovascular Research Foundation, and the Smoking Research Foundation.

Disclosures

None.

References

1. Yamashita J, Itoh H, Hirashima M, Ogawa M, Nishikawa S, Yurugi T, Naito M, Nakao K, Nishikawa S. Flk1-positive cells derived from embryonic stem cells serve as vascular progenitors. *Nature*. 2000;408:92–96.
2. Sone M, Itoh H, Yamashita J, Yurugi-Kobayashi T, Suzuki Y, Kondo Y, Nonoguchi A, Sawada N, Yamahara K, Miyashita K, Park K, Shibuya M, Nito S, Nishikawa S, Nakao K. Different differentiation kinetics of vascular progenitor cells in primate and mouse embryonic stem cells. *Circulation*. 2003;107:2085–2088.
3. Sone M, Itoh H, Kenichi Yamahara, Yamashita J, Yurugi-K T, Nonoguchi A, Suzuki Y, Chao TH, Sawada N, Fukunaga Y, Miyashita K, Park K, Oyamada N, Sawada N, Taura D, Tamura N, Kondo Y, Nito S, Suemori H, Nakatsuji N, Nishikawa N, Nakao K. Pathway for differentiation of human embryonic stem cells to vascular cell components and their potential for vascular regeneration. *Arterioscler Thromb Vasc Biol*. 2007;27:2127–2134.
4. Yamahara K, Sone M, Itoh H, Yamashita J, Yurugi-K T, Homma K, Chao TH, Miyashita K, Park K, Oyamada N, Sawada N, Taura D, Fukunaga Y, Tamura N, Nakao K. Augmentation of Neovascularization in hindlimb ischemia by combined transplantation of human embryonic stem cells-derived endothelial and mural cells. *PLOS one*. 2008;3:e1666.
5. Takahashi K, Yamanaka S. Induction of pluripotent stem cells from mouse embryonic and adult fibroblast cultures by defined factors. *Cell*. 2006;126:663–676.
6. Takahashi K, Tanabe K, Ohnuki M, Narita M, Ichisaka T, Tomoda K, Yamanaka S. Induction of pluripotent stem cells from adult human fibroblasts by defined factors. *Cell*. 2007;131:861–872.
7. Yu J, Vodyanik MA, Smuga-Otto K, Antosiewicz-Bourget J, Frane JL, Tian S, Nie J, Jonsdottir GA, Ruotti V, Stewart R, Slukvin II, Thomson JA. Induced pluripotent stem cell lines derived from human somatic cells. *Science*. 2007;318:1917–1920.
8. Fujioka T, Yasuchika K, Nakamura Y, Nakatsuji N, Suemori H. A simple and efficient cryopreservation method for primate embryonic stem cells. *Int J Dev Biol*. 2004;48:1149–1154.
9. Hirashima M, Kataoka H, Nishikawa S, Matsuyoshi N, Nishikawa S. Maturation of embryonic stem cells into endothelial cells in an in vitro model of vasculogenesis. *Blood*. 1999;93:1253–1263.
10. Nakagawa M, Koyanagi M, Tanabe K, Takahashi K, Ichisaka T, Aoi T, Okita K, Mochizuki Y, Takizawa N, Yamanaka S. Generation of induced pluripotent stem cells without Myc from mouse and human fibroblasts. *Nat Biotechnol*. 2008;26:101–106.
11. Narazaki G, Uosaki H, Teranishi M, Okita K, Kim B, Matsuoka S, Yamanaka S, Yamashita J. Directed and systematic differentiation of cardiovascular cells from mouse induced pluripotent stem cells. *Circulation*. 2008;118:498–506.

Beneficial effects of leptin on glycaemic and lipid control in a mouse model of type 2 diabetes with increased adiposity induced by streptozotocin and a high-fat diet

T. Kusakabe · H. Tanioka · K. Ebihara · M. Hirata ·
L. Miyamoto · F. Miyanaga · H. Hige · D. Aotani ·
T. Fujisawa · H. Masuzaki · K. Hosoda · K. Nakao

Received: 10 December 2008 / Accepted: 18 December 2008 / Published online: 24 January 2009
© Springer-Verlag 2009

Abstract

Aims/hypothesis We have previously demonstrated the therapeutic usefulness of leptin in lipoatrophic diabetes and insulin-deficient diabetes in mouse models and could also demonstrate its dramatic effects on lipoatrophic diabetes in humans. The aim of the present study was to explore the therapeutic usefulness of leptin in a mouse model of type 2 diabetes with increased adiposity.

Methods To generate a mouse model mimicking human type 2 diabetes with increased adiposity, we used a combination of low-dose streptozotocin (STZ, 120 µg/g body weight) and high-fat diet (HFD, 45% of energy as fat). Recombinant mouse leptin was infused chronically (20 ng [g body weight]⁻¹ h⁻¹) for 14 days using a mini-osmotic pump. The effects of leptin on food intake, body weight, metabolic variables, tissue triacylglycerol content and AMP-activated protein kinase (AMPK) activity were examined.

Results Low-dose STZ injection led to a substantial reduction of plasma insulin levels and hyperglycaemia. Subsequent HFD feeding increased adiposity and induced insulin resistance and further augmentation of hyperglycaemia. In this model mouse mimicking human type 2 diabetes (STZ/HFD), continuous leptin infusion reduced food intake and body weight and improved glucose and lipid metabolism with

enhancement of insulin sensitivity. Leptin also decreased liver and skeletal muscle triacylglycerol content accompanied by an increase of α2 AMPK activity in skeletal muscle. Pair-feeding experiments demonstrated that leptin improved glucose and lipid metabolism independently of the food intake reduction.

Conclusions/interpretation This study demonstrates the beneficial effects of leptin on glycaemic and lipid control in a mouse model of type 2 diabetes with increased adiposity, indicating the possible clinical usefulness of leptin as a new glucose-lowering drug in humans.

Keywords High-fat diet · Insulin sensitivity · Leptin · Overweight · Streptozotocin · Tissue triacylglycerol content · Type 2 diabetes

Abbreviations

AMPK AMP-activated protein kinase
GTT glucose tolerance test
HFD high-fat diet
SD standard diet
STZ streptozotocin

Introduction

Leptin is an adipocyte-derived hormone that plays a key role in regulating food intake and energy expenditure, and participates in increasing glucose metabolism [1, 2]. Leptin deficiency causes obesity, insulin resistance and diabetes in mice and humans [3–5]. We previously generated transgenic skinny mice (LepTg) overexpressing leptin under the control of the liver-specific human serum amyloid P component promoter [6]. LepTg mice showed elevated

T. Kusakabe and H. Tanioka contributed equally to this work.

T. Kusakabe · H. Tanioka · K. Ebihara (✉) · M. Hirata ·
L. Miyamoto · F. Miyanaga · H. Hige · D. Aotani · T. Fujisawa ·
H. Masuzaki · K. Hosoda · K. Nakao
Department of Medicine and Clinical Science,
Kyoto University Graduate School of Medicine,
54 Shogoin Kawahara-cho,
Sakyo-ku, Kyoto 606-8507, Japan
e-mail: kebihara@kuhp.kyoto-u.ac.jp

plasma leptin levels comparable to those of obese human individuals, providing a unique experimental model to investigate various actions of leptin [6–11]. LepTg mice exhibited increased glucose metabolism and insulin sensitivity with augmented liver and skeletal muscle insulin receptor signalling [6]. LepTg mice also exhibited increased lipid metabolism accompanied by increased lipoprotein lipase activity and clearance of triacylglycerol [7]. In addition, LepTg mice had reduced tissue triacylglycerol content along with increased energy expenditure through augmented phosphorylation of AMP-activated protein kinase (AMPK), a key enzyme that mediates the leptin effect on fatty acid β -oxidation in skeletal muscle [8, 9]. Therefore, these findings led us to hypothesise that leptin acts as a glucose-lowering drug with a lipid-lowering effect *in vivo*.

Given the glucose-lowering action of leptin, we and others have demonstrated that leptin infusion or transgenic overexpression of leptin reverses metabolic abnormalities in different mouse models of lipodystrophy [10, 12]. Recently, we and others confirmed that leptin treatment effectively reduces food intake and improves hyperglycaemia, hypertriacylglycerolaemia and fatty liver in patients with lipotrophic diabetes [13–16]. In addition, we demonstrated that leptin is useful as a glucose-lowering agent in a mouse model of insulin-deficient diabetes induced by high-dose streptozotocin (STZ) [11]. Leptin infusion reduced the dose of insulin required to improve hyperglycaemia by more than 90%, and prevented insulin-induced body weight gain in STZ-injected mice. However, the therapeutic usefulness of leptin in type 2 diabetes, a more prevalent form of diabetes, remains unclear.

In patients with type 2 diabetes, impaired insulin secretion caused by beta cell dysfunction and insulin resistance in target tissues contributes to increased blood glucose levels [17]. Patients with type 2 diabetes often exhibit dyslipidaemia and an increase of triacylglycerol content in the liver and skeletal muscle [18, 19]. Furthermore, in contrast to patients with lipotrophic diabetes and insulin-deficient diabetes who are in hypoleptinaemic states [13–16, 20], patients with type 2 diabetes often have increased adiposity and elevated leptin levels.

Previous studies have shown that low-dose STZ injection leads to the partial destruction of pancreatic beta cells and a high-fat diet (HFD) induces insulin resistance in rodents [21–23]. The degree of beta cell destruction and insulin resistance can be adjusted by dosage, duration and condition of STZ injection and HFD feeding [11, 24]. The effects of various glucose-lowering drugs (sulfonylurea, metformin, thiazolidinedione etc) have been examined in mice treated with low-dose STZ and HFD as a model of type 2 diabetes [22, 23]. In the present study, we too generated a mouse model mimicking human type 2 diabetes

using low-dose STZ and HFD to examine the effect of leptin infusion. STZ/HFD mice exhibited increased adiposity and disorders in glucose and lipid metabolism accompanied by impaired insulin secretion and insulin resistance. We report here the beneficial effects of leptin infusion on glycaemic and lipid control in this mouse model of type 2 diabetes with increased adiposity.

Methods

Animals Seven-week-old male C57BL/6J mice were purchased from Japan SLC, Shizuoka, Japan. The mice were caged individually and kept under a 12 h light–dark cycle (light on at 09:00 hours) with free access to water and standard diet (SD) (NMF, 14.6 kJ/g, 13% of energy as fat; Oriental Yeast Co., Tokyo, Japan) unless otherwise stated. Animal care and all experiments were conducted in accordance with the Guidelines for Animal Experiments of Kyoto University and were approved by the Animal Research Committee, Graduate School of Medicine, Kyoto University.

Generation of a mouse model of type 2 diabetes One week after purchase, mice were injected *i.p.* once with vehicle or low-dose STZ (120 μ g/g body weight in 10 mmol/l sodium citrate buffer, pH 4.0; Sigma-Aldrich, St Louis, MO, USA) after 4 h of fasting. After 3 weeks, the vehicle-injected mice were randomly divided and placed on SD or HFD (D12451, 19.7 kJ/g, 45% of energy as fat; Research Diets, New Brunswick, NJ, USA) (termed control and HFD mice, respectively), and the STZ-injected mice with similar degrees of hyperglycaemia and body weight were also randomly divided and placed on SD or HFD (termed STZ and STZ/HFD mice, respectively). Each group of mice was fed with either diet for 5 weeks before they were used for the leptin infusion experiment.

Leptin infusion experiments On day 0, a mini-osmotic pump (Alzet model 2002; Alza, Palo Alto, CA, USA) was implanted *s.c.* in the mid-scapular region of each mouse. The pump delivered saline or recombinant mouse leptin (Amgen, Thousand Oaks, CA, USA) (20 ng [g body weight]⁻¹ h⁻¹) *s.c.* for 14 days. SD or HFD feeding was continued during the leptin infusion experiment.

Food intake, body weight and per cent body fat Food intake was measured before and during the leptin infusion experiment. Body weight was measured on days 0 and 14. Per cent body fat was measured before the leptin infusion experiment under pentobarbital anaesthesia (Nembutal; Dainippon Sumitomo Pharma, Osaka, Japan), using a Latheta LTC-100 (Aloka, Tokyo, Japan).

Metabolic variables Blood was obtained from non-fasted mice between 15:00 and 17:00 hours. Blood glucose levels were determined by the glucose oxidase method using a reflectance glucometer (MS-GR102; Terumo, Tokyo, Japan) on days 0, 4, 7 and 14. Plasma insulin levels were measured by enzyme immunoassay with an Insulin-EIA kit (Morinaga, Tokyo, Japan). Plasma triacylglycerol, NEFA and total cholesterol levels were measured using enzymatic kits (Triglyceride E-test Wako, NEFA C-test Wako and Cholesterol E-test Wako, respectively; Wako Pure Chemicals, Osaka, Japan). Plasma leptin levels were determined using an RIA kit for mouse leptin (Linco Research Immunoassay, St Louis, MO, USA).

Glucose tolerance test (GTT) A GTT was performed on day 10. Mice were injected i.p. with 2.0 mg/g glucose after overnight fasting. Blood glucose and plasma insulin levels were measured at the indicated time points.

Liver and skeletal muscle triacylglycerol content Tissue triacylglycerol content was measured as described previously [7, 8], with modifications. Liver and quadriceps muscle were isolated at the end of the leptin infusion experiment, immediately frozen in liquid nitrogen and lipids extracted with isopropyl alcohol/heptane (1:1 vol./vol.). After evaporating the solvent, the lipids were resuspended in 99.5% (vol./vol.) ethanol, and the triacylglycerol content was measured using the Triglyceride E-test Wako kit.

Isoform-specific AMPK activity AMPK activity was determined as described previously [25, 26], with modifications.

To measure $\alpha 1$ and $\alpha 2$ isoform-specific AMPK activity in skeletal muscle, AMPK was immunoprecipitated from muscle lysates (200 μ g protein) with specific antibodies against the $\alpha 1$ - and $\alpha 2$ -subunits (Upstate Cell Signaling Solutions, Lake Placid, NY, USA) bound to Protein A-Sepharose beads, and the kinase activity of the immunoprecipitates was measured using 'SAMS' peptide and [γ - 32 P]ATP.

Pair-feeding experiments STZ or STZ/HFD mice were fed the same amount of food consumed by the corresponding leptin-infused mice on the previous day, for 14 days. A GTT was performed on day 10 of the experiment. Liver and quadriceps muscle were obtained for triacylglycerol content measurements at the end of the pair-feeding experiment.

Statistical analyses Data are expressed as means \pm SEM. Comparison between or among groups was by Student's *t* test or ANOVA with Fisher's protected least significant difference test. $p < 0.05$ was considered statistically significant.

Results

Generation of a mouse model of type 2 diabetes To generate a mouse model mimicking human type 2 diabetes with impaired insulin secretion and insulin resistance, we used low-dose STZ injection and HFD feeding. As shown in Table 1, HFD feeding effectively increased body weight, per cent body fat and plasma leptin levels in mice. With the development of adiposity, plasma insulin levels substan-

Table 1 Metabolic characteristics of the mouse model of type 2 diabetes

Variable	Mouse group			
	Control	HFD	STZ	STZ/HFD
Food intake (kJ/week)	329.0 \pm 9.3	350.7 \pm 20.0	365.3 \pm 15.1*	422.1 \pm 23.1** \dagger
Body weight (g)	26.8 \pm 0.6	34.4 \pm 1.3**	26.4 \pm 0.4	27.9 \pm 0.5 \dagger
Body fat (%)	19.8 \pm 0.7	40.6 \pm 1.1**	18.9 \pm 1.0	24.9 \pm 1.8* \dagger
Leptin (ng/ml)	4.7 \pm 0.6	26.4 \pm 1.0**	4.5 \pm 0.5	8.6 \pm 0.8** \dagger
Glucose (mmol/l)	8.3 \pm 0.2	9.2 \pm 0.4	17.5 \pm 2.3**	27.2 \pm 1.2** \dagger
Insulin (pmol/l)	160 \pm 28	315 \pm 71*	92 \pm 12*	160 \pm 38
Triacylglycerol (mmol/l)	0.66 \pm 0.09	0.86 \pm 0.08	1.11 \pm 0.14*	1.27 \pm 0.28*
NEFA (mEq/l)	0.77 \pm 0.06	1.08 \pm 0.09*	1.03 \pm 0.10*	0.99 \pm 0.09*
Total cholesterol (mmol/l)	1.48 \pm 0.08	3.61 \pm 0.18**	1.49 \pm 0.16	3.01 \pm 0.19** \dagger
Liver triacylglycerol content (mg/g tissue)	8.7 \pm 1.0	20.0 \pm 2.2**	10.2 \pm 0.9	27.1 \pm 1.7** \dagger
Skeletal muscle triacylglycerol content (mg/g tissue)	5.6 \pm 0.5	8.1 \pm 1.2*	5.4 \pm 0.5	7.8 \pm 0.8* \dagger

Values are means \pm SEM for 10–12 mice in each group

C57BL/6J mice were injected with vehicle and fed SD (control) or HFD, or injected with low-dose STZ and fed with SD (STZ) or HFD (STZ/HFD). Food intake for a week, body weight, per cent body fat, blood glucose levels and plasma levels for leptin, insulin, triacylglycerol, NEFA and total cholesterol were measured before the leptin infusion experiment. Blood samples were obtained during ad libitum feeding. Liver and skeletal muscle triacylglycerol contents were measured after the leptin infusion experiment

* $p < 0.05$, ** $p < 0.01$ vs control mice; $\dagger p < 0.05$, $\dagger\dagger p < 0.01$ vs STZ in STZ/HFD mice

tially increased, although blood glucose levels did not significantly increase, suggesting the development of insulin resistance. HFD feeding also increased plasma NEFA and total cholesterol levels, and liver and skeletal muscle triacylglycerol contents.

Low-dose STZ injection led to a substantial reduction of plasma insulin and hyperglycaemia in mice. Under these conditions, body weight, per cent body fat and plasma leptin levels were unchanged, although food intake was significantly increased. Low plasma insulin levels also led to an increase of plasma triacylglycerol and NEFA levels. Liver and skeletal muscle triacylglycerol contents were unchanged.

On the other hand, subsequent HFD feeding in low-dose STZ injected mice further increased food intake and moderately increased body weight, per cent body fat and plasma leptin levels even with the impairment of insulin secretion. Hyperglycaemia was exacerbated, although plasma insulin levels were mildly elevated, suggesting the development of insulin resistance. Increases of plasma triacylglycerol, NEFA and total cholesterol levels, and liver and skeletal muscle triacylglycerol contents, were also observed in these STZ/HFD mice.

Since STZ/HFD mice manifested increased adiposity and disorders in glucose and lipid metabolism accompanied by impaired insulin secretion and insulin resistance, we used STZ/HFD mice as a model of type 2 diabetes with increased adiposity in the present study.

Effect of leptin on food intake and body weight As shown in Fig. 1a, continuous leptin infusion elevated plasma leptin levels from baseline almost equally in control, HFD, STZ and STZ/HFD mice. Under these conditions, food intake was significantly suppressed in control, STZ and STZ/HFD mice, while that in HFD was unchanged (Fig. 1b). Consistent with food intake, body weight was effectively decreased in control, STZ and STZ/HFD mice, while that in HFD mice was unchanged (Fig. 1c).

Effect of leptin on glucose metabolism In control mice, leptin infusion did not affect blood glucose levels during ad libitum feeding but markedly decreased plasma insulin levels, suggesting the enhancement of insulin sensitivity (Fig. 2a, e). In HFD mice, leptin infusion showed no effect on either blood glucose levels or plasma insulin levels (Fig. 2b, e). On the other hand, both blood glucose levels and plasma insulin levels were effectively decreased after 2 weeks of leptin infusion in STZ and STZ/HFD mice, suggesting the improvement of insulin sensitivity (Fig. 2c–e).

To further evaluate the effect of leptin on glucose metabolism, we performed i.p. GTTs (Fig. 3). In control, STZ and STZ/HFD mice, leptin infusion significantly improved glucose tolerance with reduction of plasma

insulin levels not only in the fasting state but also after the glucose load, suggesting an improvement of insulin sensitivity. In contrast, in HFD mice, leptin infusion did not improve glucose tolerance and also did not suppress plasma insulin levels before or after glucose load.

Effect of leptin on plasma lipid profiles Leptin infusion did not affect plasma triacylglycerol, NEFA and total cholesterol levels in control mice (Fig. 4a–c). Leptin infusion also did not change plasma triacylglycerol, NEFA and total cholesterol levels in HFD mice, even though basal plasma NEFA and total cholesterol levels were elevated. In STZ mice, leptin infusion effectively decreased plasma triacylglycerol and NEFA levels, which were elevated at baseline, while leptin infusion did not affect plasma total cholesterol levels, which were not elevated at baseline. In STZ/HFD

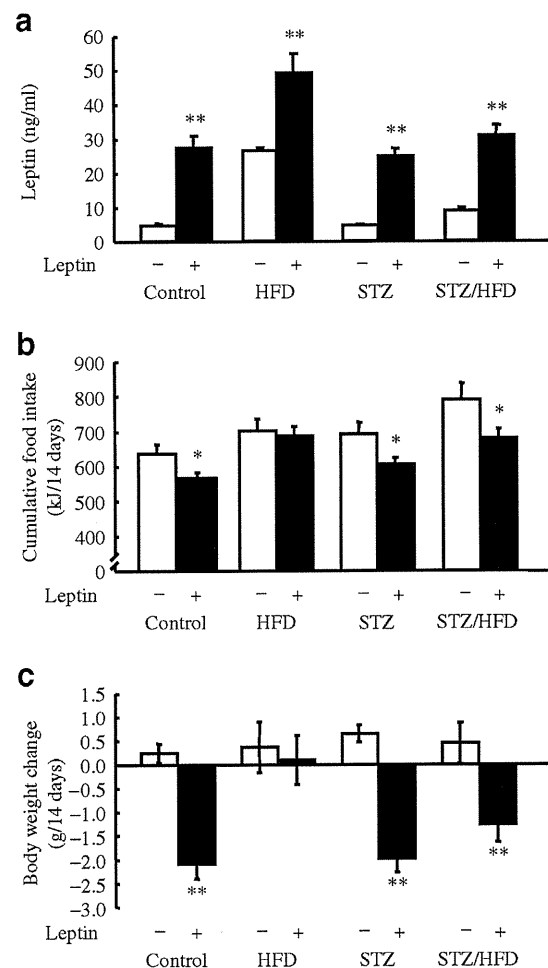


Fig. 1 Effect of leptin on leptin levels, food intake and body weight. Leptin levels on day 14 (a), cumulative food intake (b) and change in body weight (c) after 14 days of leptin infusion in control, HFD, STZ and STZ/HFD mice. Values are means \pm SEM ($n=10-17$). * $p<0.05$, ** $p<0.01$ vs corresponding saline-infused mice

mice, leptin infusion also effectively decreased plasma triacylglycerol, NEFA and total cholesterol levels, which were elevated at baseline.

Effect of leptin on liver and skeletal muscle triacylglycerol contents To assess whether the improvement of glucose metabolism by leptin infusion was associated with the reduction of triacylglycerol content in insulin-target tissues, we examined the effect of leptin infusion on liver and skeletal muscle triacylglycerol contents. As shown in Fig. 5, leptin infusion apparently decreased triacylglycerol contents of both liver and skeletal muscle in control, STZ and STZ/HFD mice, in which glucose metabolism was improved by leptin infusion. In contrast, leptin infusion decreased triacylglycerol content of neither liver nor skeletal muscle in HFD mice, in which glucose metabolism was unchanged by leptin infusion.

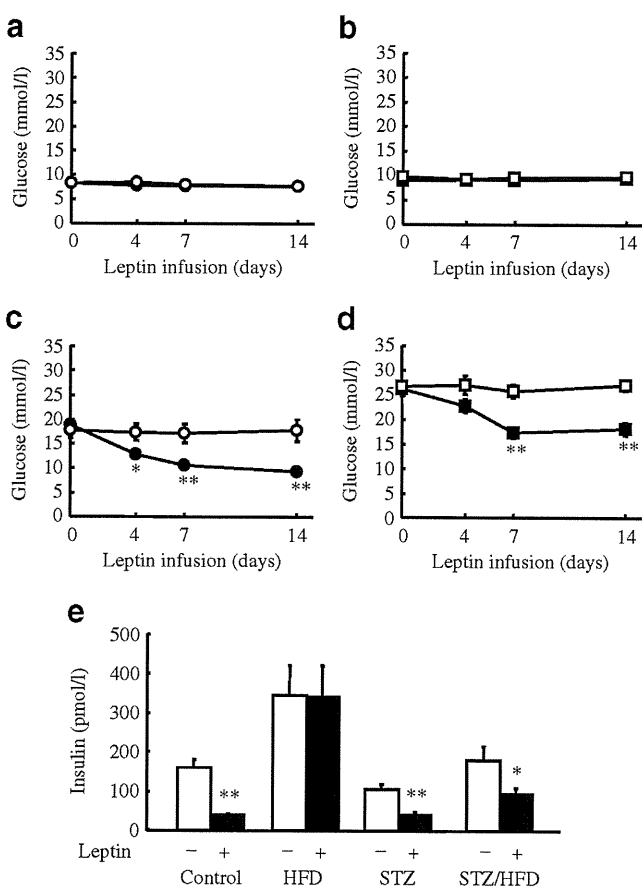


Fig. 2 Effect of leptin infusion for 14 days on blood glucose and plasma insulin levels during ad libitum feeding. Blood glucose levels on days 0, 4, 7 and 14 in control (a), HFD (b), STZ (c) and STZ/HFD mice (d). White symbols, saline-infused; black symbols, leptin-infused. e Plasma insulin levels during ad libitum feeding on day 14 in control, HFD, STZ and STZ/HFD mice. Values are means±SEM (n=10–17). *p<0.05, **p<0.01 vs corresponding saline-infused mice

Effect of leptin on AMPK activity in skeletal muscle Leptin infusion did not affect $\alpha 1$ isoform-specific AMPK activity in skeletal muscle in any group of mice (Fig. 6a). On the other hand, leptin infusion significantly increased $\alpha 2$ isoform-specific AMPK activity in skeletal muscle in control, STZ and STZ/HFD mice (Fig. 6b). However, no significant increase of $\alpha 2$ AMPK activity in skeletal muscle was observed in HFD mice.

Pair-feeding experiments We investigated whether the reduction of food intake by leptin infusion is the reason

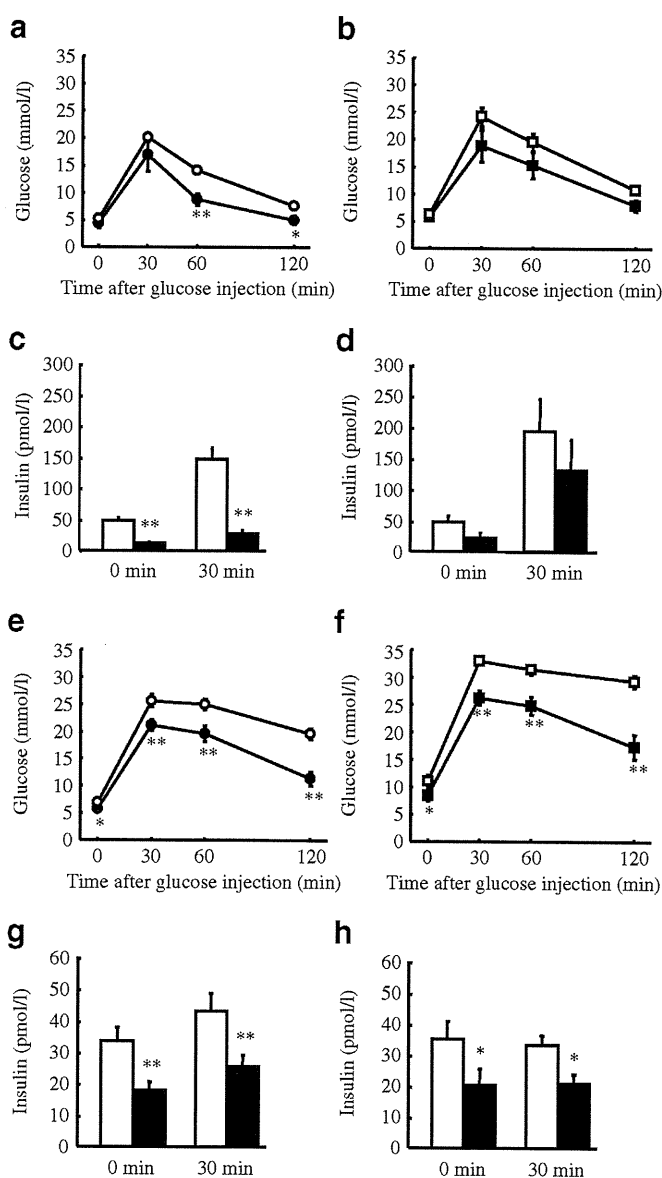


Fig. 3 Effect of leptin on glucose tolerance and insulin secretion during GTTs. Blood glucose and plasma insulin levels were measured at the indicated time points in control (a, c), HFD (b, d), STZ (e, g) and STZ/HFD mice (f, h). Values are means±SEM (n=10–17). *p<0.05, **p<0.01 vs corresponding saline-infused mice

for its efficacy in improving glucose metabolism. We paired STZ and STZ/HFD mice the same amount of food consumed by the corresponding leptin-infused mice on the previous day. Pair-feeding did not improve glucose tolerance in GTTs in STZ and STZ/HFD mice (data not shown). Moreover, when compared with basal values (Table 1), no significant decrease of liver and skeletal muscle triacylglycerol contents was observed in pair-fed STZ and STZ/HFD mice (liver triacylglycerol content: 8.3 ± 1.2 and 30.0 ± 5.6 mg/g tissue; skeletal muscle triacylglycerol content: 5.4 ± 0.5 and 6.6 ± 0.5 mg/g tissue, in pair-fed STZ and STZ/HFD mice, respectively, $n=5$ in each group of mice), in contrast to the corresponding leptin-infused mice (Fig. 5).

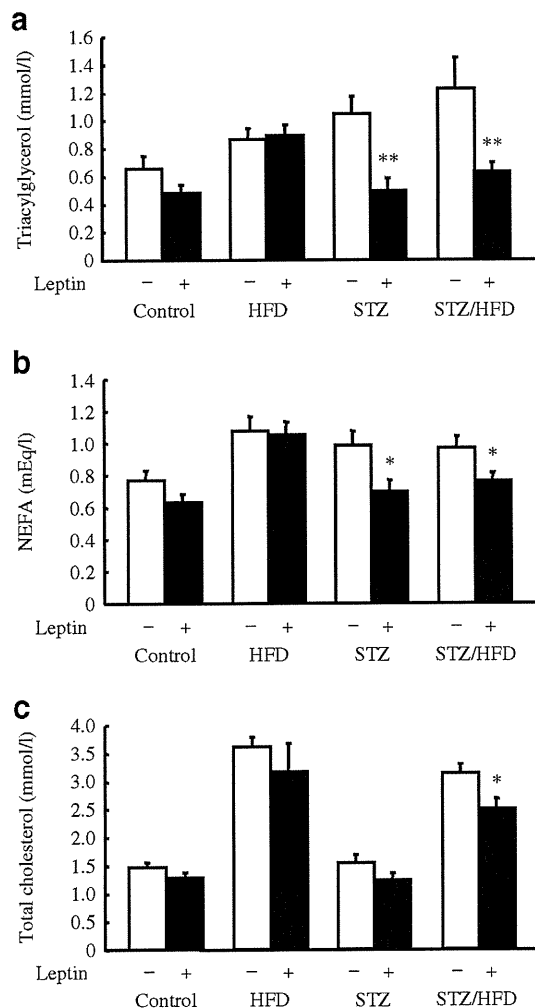


Fig. 4 Effect of leptin on plasma lipid profiles. Plasma triacylglycerol (a), NEFA (b) and total cholesterol levels (c) during ad libitum feeding on day 14 in control, HFD, STZ and STZ/HFD mice. Values are means \pm SEM ($n=10-17$). * $p<0.05$, ** $p<0.01$ vs corresponding saline-infused mice

Discussion

The effectiveness of leptin treatment in diabetes has been reported in patients with leptin deficiency and lipodystrophy and in amenorrhoea in patients with hypothalamic hypogonadism caused by low body weight [5, 13–16, 27]. These patients are in hypoleptinaemic states, and hypoleptinaemia is involved in the pathophysiology of their diseases. However, whether leptin treatment is effective in normo- or hyperleptinaemic states has not been fully examined. The aim of the present study was to explore the therapeutic usefulness of leptin in type 2 diabetes, which is often accompanied by increased adiposity. Type 2 diabetes develops as a result of insulin resistance in target tissues and impaired insulin secretion, accompanied by increased adiposity. To generate a mouse model mimicking human type 2 diabetes, we used a combination of low-dose STZ and HFD. Although high-dose STZ injection generally reduces body weight, with a marked reduction of insulin levels [16], low-dose STZ used in this study did not reduce body weight. In addition, subsequent HFD feeding in low-dose STZ injected mice could increase body weight even

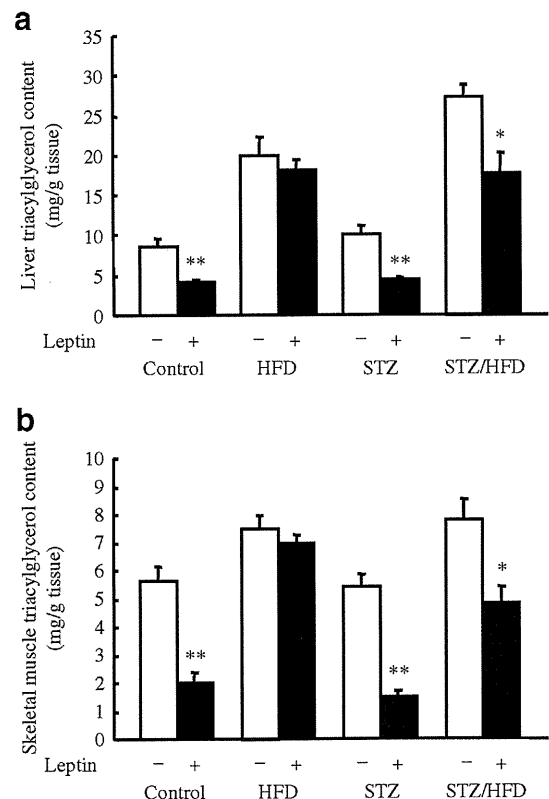


Fig. 5 Effect of leptin on liver and skeletal muscle triacylglycerol contents. Liver (a) and skeletal muscle (b) triacylglycerol contents on day 14 in STZ and STZ/HFD mice. Values are means \pm SEM ($n=10-13$). * $p<0.05$, ** $p<0.01$ vs corresponding saline-infused mice

with the impairment of insulin secretion in this study. Consistent with the increase in body weight and per cent body fat, STZ/HFD mice showed a nearly twofold increase in plasma leptin levels compared with control mice (Table 1). In humans, plasma leptin levels positively correlated with BMI, and a twofold increase in plasma leptin levels corresponds to a BMI in the range of 25–30 kg/m² [28, 29]. According to recent clinical studies, the average BMI in patients with type 2 diabetes is within this overweight range [30–32]. HFD mice showed a larger increase in adiposity and plasma leptin levels than did STZ/HFD mice. However, unlike STZ/HFD mice, HFD mice did not develop hyperglycaemia, because of compensatory hyperinsulinaemia. Therefore, we used STZ/HFD mice as an appropriate model to examine the efficacy of leptin in type 2 diabetes with increased adiposity.

The present study showed that the effect of leptin on food intake and body weight was attenuated in obese HFD mice (Fig. 1b, c). In general, in human obesity and rodent models of diet-induced obesity, even though leptin levels rise proportionally with adiposity, the increased leptin fails to suppress the progression of obesity. Moreover, obese humans and rodents are weakly responsive to exogenously administered leptin in terms of body weight reduction

[33, 34]. This leptin ineffectiveness is called leptin resistance. The present study also showed that the effect of leptin on glucose and lipid metabolism was attenuated in obese HFD mice (Figs 2, 3, 4 and 5). In contrast, even under HFD feeding, leptin effectively improved glucose and lipid metabolism in STZ/HFD mice. Impaired insulin secretion caused by STZ injection could reduce the effect of HFD feeding on the development of obesity in STZ/HFD mice. As a result, leptin resistance could be mild, if any, in STZ/HFD mice. The present study demonstrated that leptin could be a glucose-lowering drug for the treatment of type 2 diabetes with impaired insulin secretion.

Fat accumulation in insulin target tissues is considered to be one of the causes of insulin resistance, and is called lipotoxicity [35, 36]. Indeed, HFD and STZ/HFD mice exhibited insulin resistance and increased liver and skeletal muscle triacylglycerol contents (Table 1). In the present study, we investigated an association between the improvement of glucose metabolism by leptin infusion and the reduction of liver and skeletal muscle triacylglycerol contents. Leptin infusion enhanced insulin sensitivity in control, STZ and STZ/HFD mice, in which it decreased liver and skeletal muscle triacylglycerol contents (Figs 3 and 5). In contrast, leptin infusion did not improve insulin resistance in HFD mice, in which it did not decrease liver and skeletal muscle triacylglycerol contents. Moreover, pair-feeding neither improved glucose tolerance nor decreased the liver and skeletal muscle triacylglycerol contents in STZ and STZ/HFD mice. These results suggest that the improvement of glucose metabolism by leptin infusion is associated with a reduction in liver and skeletal muscle triacylglycerol contents.

Leptin has been shown to selectively stimulate activation of the $\alpha 2$ catalytic subunit of AMPK in skeletal muscle [37]. AMPK is a key enzyme that mediates the leptin effect on fatty acid β -oxidation in skeletal muscle. In the present study, leptin infusion effectively decreased skeletal muscle triacylglycerol content in control, STZ and STZ/HFD mice (Fig. 5b), in which it increased $\alpha 2$ AMPK activity in skeletal muscle (Fig. 6b). In contrast, leptin infusion did not decrease skeletal muscle triacylglycerol content in HFD mice (Fig. 5b), in which it did not increase $\alpha 2$ AMPK activity in skeletal muscle (Fig. 6b). Increased fatty acid β -oxidation through $\alpha 2$ AMPK activation in skeletal muscle is considered to be one of the mechanisms by which leptin decreases skeletal muscle triacylglycerol content [9].

The present study also showed that leptin infusion effectively improved hyperlipidaemia in STZ and STZ/HFD mice (Fig. 4). Increased lipoprotein lipase activity, increased clearance of triacylglycerol [7], reduction of triacylglycerol synthesis by controlling key transcription factors [38] and increased energy expenditure through fatty acid β -oxidation have been reported as mechanisms by

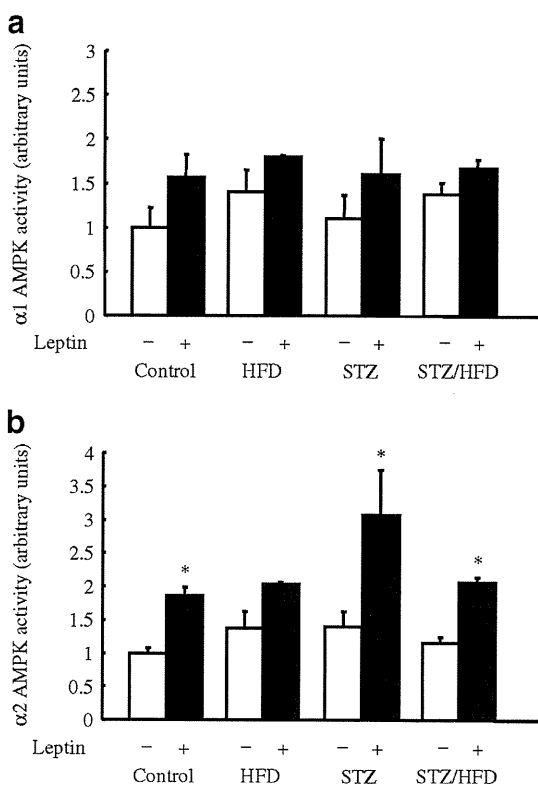


Fig. 6 Effect of leptin on isoform-specific AMPK activity in skeletal muscle. $\alpha 1$ AMPK activity (a) and $\alpha 2$ AMPK activity (b) on day 14 in soleus muscle of STZ and STZ/HFD mice. Values are means \pm SEM ($n=4-5$). * $p<0.05$ vs corresponding saline-infused mice

which leptin decreases plasma triacylglycerol levels. The present study demonstrated activation of $\alpha 2$ AMPK activity by leptin infusion in skeletal muscle (Fig. 6b), which might contribute to increased energy expenditure in our leptin-infused STZ and STZ/HFD mice. It is also well known that impaired insulin action induces hyperlipidaemia [39]. It is also possible that leptin improved hyperlipidaemia by enhancement of insulin sensitivity in the present study.

The present study demonstrated that pair-feeding neither improved glucose tolerance nor decreased liver and skeletal muscle triacylglycerol contents in STZ and STZ/HFD mice. Previously, we and others have demonstrated that food intake reduction alone was insufficient for improving glucose and lipid metabolism [6, 10, 12]. It has also been reported that fasting insulin and triacylglycerol levels increased within several days after withdrawal of leptin administration even though the level of food intake remained constant in the patients with lipodystrophy [13]. Furthermore, it has been demonstrated that leptin administration decreases liver and skeletal muscle triacylglycerol contents in patients with lipodystrophy [40]. These results indicate that leptin improves glucose and lipid metabolism independently of the food intake reduction.

With the dose of leptin used in the present study, the plasma leptin levels in STZ/HFD mice increased to the levels of obese HFD mice (mean leptin levels in leptin-infused STZ/HFD mice, 30.8 ng/ml) (Fig. 1a), which can be seen in human obese individuals. In our clinical research on leptin-replacement therapy in patients with generalised lipodystrophy, the peak plasma leptin levels of the 400% dose under the protocol of once-daily injections was 34.5 ± 2.1 (mean \pm SE) ng/ml, and the therapy was well tolerated without any adverse effects for about 5 years [15]. In addition, higher leptin levels were obtained in the obese human clinical trial [33]. Therefore, the leptin levels achieved with the dose used in the present study could be clinically applied in humans.

In conclusion, the present study demonstrates that leptin therapy improves glucose and lipid metabolism and enhances insulin sensitivity in a mouse model of type 2 diabetes with an overweight range of adiposity. Our findings indicate that leptin could be a new glucose-lowering drug for the treatment of type 2 diabetes in humans.

Acknowledgements We thank M. Nagamoto for technical assistance and Y. Koyama for secretarial assistance. This work was supported in part by research grants from the Ministry of Education, Culture, Sports, Science and Technology of Japan; the Ministry of Health, Labour and Welfare of Japan; the Takeda Medical Research Foundation and Japan Foundation of Applied Enzymology; and the ONO Medical Research Foundation.

Duality of interest The authors declare that there is no duality of interest associated with this manuscript.

References

- Halaas JL, Gajiwala KS, Maffei M (1995) Weight-reducing effects of the plasma protein encoded by the obese gene. *Science* 269:543–546
- Friedman JM, Halaas JL (1998) Leptin and the regulation of body weight in mammals. *Nature* 395:763–770
- Muzzin P, Eisensmith RC, Copeland KC, Woo SLC (1996) Correction of obesity and diabetes in genetically obese mice by leptin gene therapy. *Proc Natl Acad Sci U S A* 93:14804–14808
- Montague CT, Farooqi IS, Whitehead JP (1997) Congenital leptin deficiency is associated with severe early-onset obesity in humans. *Nature* 387:903–908
- Licinio J, Caglayan S, Ozata M (2004) Phenotypic effects of leptin replacement on morbid obesity, diabetes mellitus, hypogonadism, and behavior in leptin-deficient adults. *Proc Natl Acad Sci U S A* 101:4531–4536
- Ogawa Y, Masuzaki H, Hosoda K (1999) Increased glucose metabolism and insulin sensitivity in transgenic skinny mice overexpressing leptin. *Diabetes* 48:1822–1829
- Matsuoka N, Ogawa Y, Masuzaki H (2001) Decreased triglyceride-rich lipoproteins in transgenic skinny mice overexpressing leptin. *Am J Physiol Endocrinol Metab* 280:E334–E339
- Tanaka T, Masuzaki H, Yasue S (2007) Central melanocortin signaling restores skeletal muscle AMP-activated protein kinase phosphorylation in mice fed a high-fat diet. *Cell Metabolism* 5:395–402
- Tanaka T, Hidaka S, Masuzaki H (2005) Skeletal muscle AMP-activated protein kinase phosphorylation parallels metabolic phenotype in leptin transgenic mice under dietary modification. *Diabetes* 54:2365–2374
- Ebihara K, Ogawa Y, Masuzaki H (2001) Transgenic overexpression of leptin rescues insulin resistance and diabetes in a mouse model of lipodystrophic diabetes. *Diabetes* 50:1440–1448
- Miyayama F, Ogawa Y, Ebihara K (2003) Leptin as an adjunct of insulin therapy in insulin-deficient diabetes. *Diabetologia* 46:1329–1337
- Shimomura I, Hammer RE, Ikemoto S, Brown MS, Goldstein JL (1999) Leptin reverses insulin resistance and diabetes mellitus in mice with congenital lipodystrophy. *Nature* 401:73–76
- Oral EA, Simha V, Ruiz E (2002) Leptin-replacement therapy for lipodystrophy. *N Engl J Med* 346:570–578
- Ebihara K, Masuzaki H, Nakao K (2004) Long-term leptin-replacement therapy for lipodystrophic diabetes. *N Engl J Med* 351:615–616
- Ebihara K, Kusakabe T, Hirata M (2007) Efficacy and safety of leptin-replacement therapy and possible mechanisms of leptin actions in patients with generalized lipodystrophy. *J Clin Endocrinol Metab* 92:532–541
- Beltrand J, Beregszaszi M, Chevenne D (2007) Metabolic correction induced by leptin replacement treatment in young children with Berardinelli–Seip congenital lipodystrophy. *Pediatrics* 120:e291–e296
- Taylor SI (1999) Deconstructing type 2 diabetes. *Cell* 97:9–12
- Ishii M, Yoshioka Y, Ishida W (2005) Liver fat content measured by magnetic resonance spectroscopy at 3.0 tesla independently correlates with plasminogen activator inhibitor-1 and body mass index in type 2 diabetic subjects. *Tohoku J Exp Med* 206:23–30
- Sinha R, Dufour S, Petersen KF (2002) Assessment of skeletal muscle triglyceride content by ^1H nuclear magnetic resonance spectroscopy in lean and obese adolescents: relationships to insulin sensitivity, total body fat, and central adiposity. *Diabetes* 51:1022–1027
- Kiess W, Anil M, Blum WF (1998) Serum leptin levels in children and adolescents with insulin-dependent diabetes mellitus in relation to metabolic control and body mass index. *Eur J Endocrinol* 138:501–509

21. Ding SY, Shen ZF, Chen YT, Sun SJ, Liu Q, Xie MZ (2005) Pioglitazone can ameliorate insulin resistance in low-dose streptozotocin and high sucrose-fat diet induced obese rats. *Acta Pharmacol Sin* 26:575–580
22. Luo J, Quan J, Tsai J (1998) Nongenetic mouse models of non-insulin-dependent diabetes mellitus. *Metabolism* 47:663–668
23. Mu J, Woods J, Zhou YP (2006) Chronic inhibition of dipeptidyl peptidase-4 with a sitagliptin analog preserves pancreatic β -cell mass and function in a rodent model of type 2 diabetes. *Diabetes* 55:1695–1704
24. Shertzer HG, Schneider SN, Kendig EL, Clegg DJ, D'Alessio DA, Genter MB (2008) Acetaminophen normalizes glucose homeostasis in mouse models for diabetes. *Biochem Pharmacol* 75:1402–1410
25. Miyamoto L, Toyoda T, Hayashi T (2007) Effect of acute activation of 5'-AMP-activated protein kinase on glycogen regulation in isolated rat skeletal muscle. *J Appl Physiol* 102:1007–1013
26. Toyoda T, Tanaka S, Ebihara K (2006) Low-intensity contraction activates the α 1-isoform of 5'-AMP-activated protein kinase in rat skeletal muscle. *Am J Physiol Endocrinol Metab* 290:E583–E590
27. Welt CK, Chan JL, Bullen J (2004) Recombinant human leptin in women with hypothalamic amenorrhea. *N Engl J Med* 351:987–997
28. Buettner R, Bollheimer LC, Zietz B (2002) Definition and characterization of relative hypo- and hyperleptinemia in a large Caucasian population. *J Endocrinol* 175:745–756
29. Peltz G, Sanderson M, Pérez A, Sexton K, Ochoa Casares D, Fadden MK (2007) Serum leptin concentration, adiposity, and body fat distribution in Mexican-Americans. *Arch Med Res* 38:563–570
30. Widjaja A, Stratton IM, Horn R, Holman RR, Tuner R, Brabant G (1997) UKPDS 20: Plasma leptin, obesity, and plasma insulin in type 2 diabetic subjects. *J Clin Endocrinol Metab* 82:654–657
31. Sone H, Yoshimura Y, Tanaka S (2007) Cross-sectional association between BMI, glycemic control and energy intake in Japanese patients with type 2 diabetes. Analysis from the Japan Diabetes Complications Study. *Diabetes Res Clin Pract* 77S:S23–S29
32. Sone H, Ito H, Ohashi Y, Akanuma Y, Yamada N, Japan Diabetes Complications Study (JDACS) Group (2003) Obesity and type 2 diabetes in Japanese patients. *Lancet* 361:85
33. Heymsfield SB, Greenberg AS, Fujioka K (1999) Recombinant leptin for weight loss in obese and lean adults: a randomized, controlled, dose-escalation trial. *JAMA* 282:1568–1575
34. El-Haschimi K, Pierroz DD, Hileman SM, Bjorbaek C, Flier JS (2000) Two defects contribute to hypothalamic leptin resistance in mice with diet-induced obesity. *J Clin Invest* 105:1827–1832
35. Schulman GI (2000) Cellular mechanisms of insulin resistance. *J Clin Invest* 106:171–176
36. Unger RH (2003) Minireview: Weapons of lean body mass destruction: the role of ectopic lipids in the metabolic syndrome. *Endocrinology* 144:5159–5165
37. Minokoshi Y, Kim YB, Peroni OD (2002) Leptin stimulates fatty-acid oxidation by activating AMP-activated protein kinase. *Nature* 415:339–343
38. Cohen P, Miyazaki M, Socci ND (2002) Role for stearyl-CoA desaturase-1 in leptin-mediated weight loss. *Science* 297:240–243
39. Reaven GM (2005) Why Syndrome X? From Harold Himsworth to the insulin resistance syndrome. *Cell Metab* 1:9–14
40. Petersen KF, Oral EA, Dufour S (2002) Leptin reverses insulin resistance and hepatic steatosis in patients with severe lipodystrophy. *J Clin Invest* 109:1345–1350

Systemic Administration of C-Type Natriuretic Peptide as a Novel Therapeutic Strategy for Skeletal Dysplasias

Akihiro Yasoda, Hidetomo Kitamura, Toshihito Fujii, Eri Kondo, Naoaki Murao, Masako Miura, Naotetsu Kanamoto, Yasato Komatsu, Hiroshi Arai, and Kazuwa Nakao

Department of Medicine and Clinical Science (A.Y., T.F., E.K., M.M., N.K., Y.K., H.A., K.N.), Kyoto University Graduate School of Medicine, Sakyo-ku, Kyoto 606-8507, Japan; and Fuji-Gotemba Research Laboratories (H.K., N.M.), Chugai Pharmaceutical Company, Limited, Gotemba, Shizuoka 412-8513, Japan

Skeletal dysplasias are a group of genetic disorders characterized by severe impairment of bone growth. Various forms of them add to produce a significant morbidity and mortality, yet no efficient drug therapy has been developed to date. We previously demonstrated that C-type natriuretic peptide (CNP), a member of the natriuretic peptide family, is a potent stimulator of endochondral bone growth. Furthermore, we exhibited that targeted overexpression of a CNP transgene in the growth plate rescued the impaired bone growth observed in a mouse model of achondroplasia (Ach), the most frequent form of human skeletal dysplasias, leading us to propose that CNP may prove to be an effective treatment for this disorder. In the present study, to elucidate whether or not the systemic administration of CNP is a novel drug therapy for skeletal dysplasias, we have investigated the effects of plasma CNP on impaired bone growth in Ach mice that specifically overexpress CNP in the liver under the control of human serum amyloid P component promoter or in those treated with a continuous CNP infusion system. Our results demonstrated that increased plasma CNP from the liver or by iv administration of synthetic CNP-22 rescued the impaired bone growth phenotype of Ach mice without significant adverse effects. These results indicate that treatment with systemic CNP is a potential therapeutic strategy for skeletal dysplasias, including Ach, in humans. (*Endocrinology* 150: 3138–3144, 2009)

Skeletal dysplasias are a group of genetic disorders characterized by impairment of bone growth. They comprise a diverse group of disorders that, although individually are relatively rare, together affect a large number of individuals and cause significant morbidity and mortality (1). Achondroplasia (Ach) is the most common skeletal dysplasia with a birth prevalence of approximately one of every 10,000 births (2). Recent studies in molecular genetics demonstrated that Ach is caused by constitutive active mutation of fibroblast growth factor receptor 3 (FGFR3), which results in disturbed proliferation and differentiation of growth plate chondrocytes followed by impaired endochondral bone growth (2, 3). Current therapy for Ach generally is limited to distraction osteogenesis (4), an orthopedic procedure (5). Although distraction osteogenesis provides some benefit, it is associated with a significant physical burden and time commitment from patients. As a trial for another treatment

of Ach, administration of GH was performed (6) but proved to have minimal effect. New therapeutic strategies for Ach are ardently expected at present.

We previously disclosed that the C-type natriuretic peptide (CNP) and its receptor, guanylyl cyclase-B (GC-B) system is the potent stimulatory system for endochondral bone growth. Both CNP and GC-B are expressed in proliferative and pre-hypertrophic chondrocyte layers of growth plate, and mice with targeted overexpression of CNP in cartilage exhibit prominent skeletal overgrowth (7). On the contrary, mice depleted with CNP (8) or GC-B (9) are dwarf due to impaired endochondral bone growth. Furthermore, loss-of-function mutations affecting GC-B are demonstrated to cause one form of autosomal recessive human skeletal dysplasia, acromesomelic dysplasia, type Maroteaux (AMDM) (10, 11), indicating that the CNP/GC-B system is crucial for endochondral bone growth in humans as well as in mice.

ISSN Print 0013-7227 ISSN Online 1945-7170

Printed in U.S.A.

Copyright © 2009 by The Endocrine Society

doi: 10.1210/en.2008-1676 Received December 10, 2008. Accepted March 3, 2009.

First Published Online March 12, 2009

Abbreviations: AMDM, Acromesomelic dysplasia, type Maroteaux; Ach, achondroplasia; CNP, C-type natriuretic peptide; CNP-LI, CNP-like immunoreactivity; FGFR3, fibroblast growth factor receptor 3; GC-B, guanylyl cyclase-B; SAP, serum amyloid P component.

In our previous report, we demonstrated that cartilage-specific overexpression of a CNP transgene rescues the impaired endochondral bone growth of a mouse model of Ach with targeted expression of constitutive active FGFR3 in cartilage (12) (hereafter called Ach mice) by restoring the decreased matrix production in Ach growth plates through inhibition of FGFR3-mediated MAPK signaling pathway (7). To elucidate whether or not the systemic administration of CNP is a novel drug therapy for skeletal dysplasias, here we investigated the effects of plasma CNP on impaired bone growth in Ach mice that specifically overexpress CNP in the liver under the control of human serum amyloid P component (SAP) promoter or in those treated with a continuous CNP infusion system. Our results indicate that treatment with systemic CNP can be a potential therapeutic strategy for skeletal dysplasias, including Ach, in humans.

Materials and Methods

Mice

Ach mice (FVB background) were created as reported previously (12), whereas the methods used to generate SAP-CNP-Tg mice (C57BL/6J background) will be reported in detail elsewhere (Kake T., H. Kitamura, Y. Adachi, T. Yoshiaki, T. Tachibe, Y. Kawase, K. Jishage, A. Yasoda, M. Mukoyama, and K. Nakao, submitted for publication). Ach mice and SAP-CNP-Tg mice were crossed to generate double-transgenic Ach/SAP-CNP-Tg mice; female F1 progeny were used for the analyses. ICR mice were purchased from Shimizu Experimental Supplies (Kyoto, Japan). Animal care and all experiments were conducted in accordance with the institutional guidelines of Kyoto University Graduate School of Medicine.

Measurement of plasma CNP concentrations

Plasma CNP-22 concentrations were measured using liquid chromatography-mass spectrometry (13). Because the lower limit of detection of liquid chromatography-mass spectrometry was 0.2 ng/ml plasma CNP-22, RIAs for CNP were performed (14) when CNP concentrations were less than 0.2 ng/ml. The cross-reactivity of CNP-53 in the RIA was about 30% on a molar basis.

Administration of CNP to mice

CNP-22 was purchased from the Peptide Institute (Minoh, Japan) and continuously infused into mice via the jugular vein using a mouse continuous infusion system (Instech Laboratories, Plymouth Meeting, PA) equipped with a syringe pump (Harvard Apparatus, Holliston, MA). Female ICR mice or Ach mice (3 wk old) were treated with vehicle or CNP at the indicated doses for 3 or 4 wk.

Skeletal analysis and histology

Skeletal analysis was performed as previously described (15). Briefly, mice were subjected to soft x-ray analysis (30 kVp, 5 mA for 1 min; Softron Type SRO-M5; Softron, Tokyo, Japan), and the lengths of the bones were measured on the soft x-ray film. To evaluate the bone mineral density at the midshaft of the femora, femora of ICR mice at the end of the treatment period were subjected to peripheral quantitative computed tomography using an XCT Research SA instrument (Stratec Medizintechnik GmbH, Pforzheim, Germany), as previously reported (7). For histological analysis, bones were fixed in 10% formalin in 0.01 M PBS (pH 7.4), decalcified in 5% formic acid, and embedded in paraffin. Five-micrometer-thick sections were sliced and stained with safranin-O, hematoxylin, and eosin. Immunohistochemical studies were performed by using rabbit anti-type II collagen antibody (LSL, Tokyo, Japan), rabbit anti-type X collagen antibody (LSL), goat anti-PTH/PTHrP receptor an-

tibody (Santa Cruz Biotechnology, Santa Cruz, CA), goat anti-Indian hedgehog antibody (Santa Cruz Biotechnology), or goat anti-Runx2 antibody (Santa Cruz Biotechnology), and the methods will be described in detail elsewhere (Kake T., H. Kitamura, Y. Adachi, T. Yoshiaki, T. Tachibe, Y. Kawase, K. Jishage, A. Yasoda, M. Mukoyama, and K. Nakao, submitted for publication).

Statistical analysis

Data are expressed as means \pm SEM or SD. The statistical significance of differences between mean values was assessed using Student's *t* test.

Results

Rescue of impaired bone growth of Ach mice by blood-borne CNP from a CNP transgene under the control of SAP promoter

To confirm whether or not blood-borne CNP effectively stimulates endochondral bone growth in mice, we developed transgenic mice in which CNP was overexpressed in the liver under the control of human SAP promoter; compared with wild-type mice, these mice showed increased concentrations of plasma CNP-like immunoreactivity (CNP-LI) (Kake T., H. Kitamura, Y. Adachi, T. Yoshiaki, T. Tachibe, Y. Kawase, K. Jishage, A. Yasoda, M. Mukoyama, and K. Nakao, submitted for publication). Two transgenic mouse lines showed phenotypes similar to those of transgenic mice that specifically overproduce CNP in the growth plate; the mouse line with the milder phenotypes was used as the SAP-CNP transgenic mice (SAP-CNP-Tg mouse) in the present study. The plasma CNP-LI concentration was 7.5 pg/ml in SAP-CNP-Tg mice, whereas it was less than 4 pg/ml in wild-type mice. In SAP-CNP-Tg mice, no significant effects were observed for hemodynamic parameters, including systolic blood pressure [104.7 ± 2.0 and 107.2 ± 2.0 (mean \pm SD) mm Hg in SAP-CNP-Tg and wild-type mice, respectively], or for blood biochemical parameters, including electrolyte concentrations (Table 1). SAP-CNP-Tg mice exhibited skeletal overgrowth, and at the age of 10 wk, each bone formed through endochondral ossification was longer and its growth plate was wider in SAP-CNP-Tg mice than in their wild-type littermates. Nevertheless, immunohistochemical analyses of tibial growth plates from 10-wk-old mice revealed that the expression patterns and intensities of chondrocyte differentiation markers including type II and X collagens, PTH/PTHrP receptor, Indian hedgehog, and Runx2 are not changed in the SAP-CNP-Tg growth plate compared with those in the wild-type growth plate (Kake T., H. Kitamura, Y. Adachi, T. Yoshiaki, T. Tachibe, Y. Kawase, K. Jishage, A. Yasoda, M. Mukoyama, and K. Nakao, submitted for publication).

Ach mice crossed with SAP-CNP-Tg mice (double-transgenic Ach/SAP-CNP-Tg mice) showed no marked difference in body length at birth compared with Ach mice, probably because the SAP-CNP transgene was first expressed after birth as previously reported (16). Nevertheless, at the age of 2 wk, Ach/SAP-CNP-Tg mice were longer than their Ach littermates and were similar in length to their wild-type littermates after 6 wk of age (Fig. 1, A and B). Soft x-ray analysis demonstrated that the impaired growth of bones formed via endochondral ossification, such as the humerus, radius, ulna, femur, and tibia, was rescued

TABLE 1. Biochemical parameters of SAP-CNP-Tg mice

	TP (g/dl)	Alb (g/dl)	AST (IU/liter)	ALT (IU/liter)	Al-P (IU/liter)	F-Cho (mg/dl)	T-Cho (mg/dl)	TG (mg/dl)	Glu (mg/dl)	Ca (mg/dl)	BUN (mg/dl)	IP (mg/dl)	CRE (mg/dl)	Na (mEq/liter)	K (mEq/liter)	Cl (mEq/liter)	
SAP-CNP-Tg																	
Mean	4.96	2.95	39.08	5.29	482.57 ^a	17.36	65	15.64	242.3	3.15	24.56	7.55	0.31	147.24	5.68	105.31	
SD	0.3	0.17	7.1	1.59	271.92	5.62	12.64	8.82	49.62	1.67	1.66	1.44	0.09	2.06	1.16	2.07	
Wild type																	
Mean	5.06	2.96	39.71	6.14	210.14	19.71	69.21	20.79	259.5	3.52	22.6	7.32	0.34	146.79	5.25	105.64	
SD	0.28	0.32	7.92	1.83	106.49	3.1	10.18	9.5	33.59	1.57	4.78	1.36	0.02	1.84	1.31	2.45	

For SAP-CNP-Tg and wild-type mice, n = 8 each. TP, Total protein; Alb, albumin; AST, aspartate aminotransferase; ALT, alanine aminotransferase; Al-P, alkaline phosphatase; F-Cho, free cholesterol; T-Cho, total cholesterol; TG, triglyceride; Glu, glucose; BUN, blood urea nitrogen; IP, inorganic phosphorus; CRE, creatinine.

^a P < 0.01, significant difference against wild type (unpaired t test).

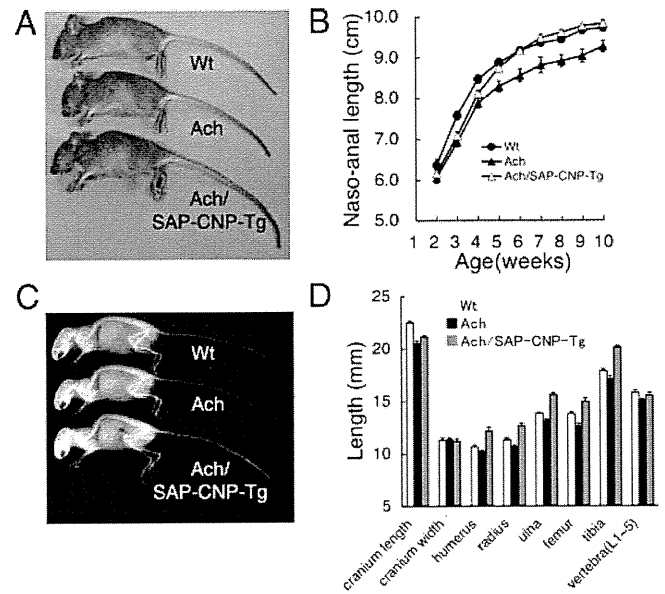


FIG. 1. Crossing Ach mice with SAP-CNP-Tg mice rescued the Ach skeletal phenotype. A, Gross appearances of 10-wk-old wild-type (Wt), Ach, and Ach/SAP-CNP-Tg mice; B, growth curves of Wt, Ach, and Ach/SAP-CNP-Tg mice from 2–10 wk after birth (●, Wt mice; ▲, Ach mice; △, Ach/SAP-CNP-Tg mice); C, soft x-ray picture of 10-wk-old Wt, Ach, and Ach/SAP-CNP-Tg mice; D, bone lengths of mice at the age of 10 wk measured on soft x-ray films (white bars, Wt mice; black bars, Ach mice; gray bars, Ach/SAP-CNP-Tg mice).

in Ach/SAP-CNP-Tg mice; indeed, these bones were longer in Ach/SAP-CNP-Tg mice than in wild-type mice (Fig. 1, C and D). As for cranium, the shortness of longitudinal length in Ach mice was not recovered in Ach/SAP-CNP-Tg mice. The width, of which the growth is dependent on membranous ossification, did not differ among the three genotypes (Fig. 1D). Histological analysis revealed that the narrowed growth plate observed in Ach mice was not found in Ach/SAP-CNP-Tg mice (Fig. 2). Chondrocytes in the growth plate, and in particular hypertrophic chondrocytes, were smaller in Ach mice than in wild-type mice, whereas in Ach/SAP-CNP-Tg mice, they were larger than in wild-

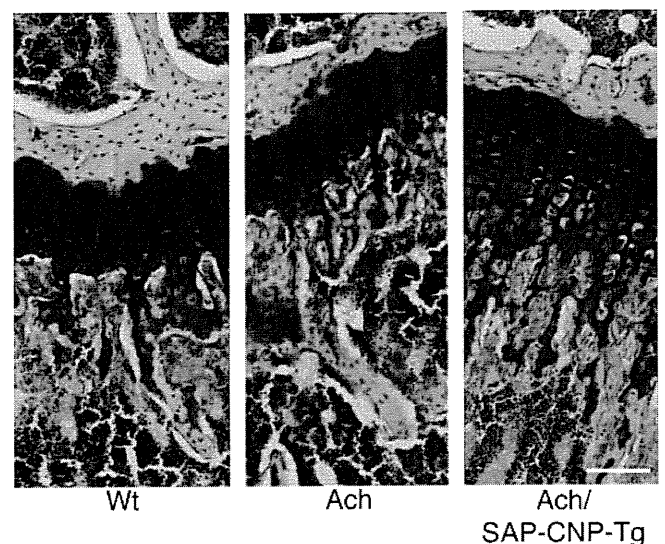


FIG. 2. Histological analysis of tibial growth plates from 4-month-old wild-type (Wt), Ach, and Ach/SAP-CNP-Tg mice. Samples were stained with safranin-O, hematoxylin, and eosin. Scale bar, 100 μm.

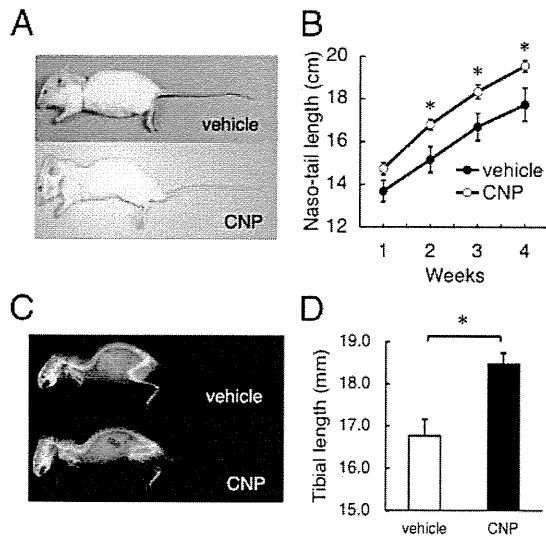


FIG. 3. Effects of iv administration of synthetic CNP-22 on bone growth. Continuous administration of vehicle or CNP-22 to female ICR mice was performed for 4 wk beginning 3 wk after birth. A, Gross appearances of vehicle-treated (upper panel) or CNP-22-treated at a dose of 5 $\mu\text{g}/\text{kg} \cdot \text{min}$ (lower panel) ICR mice at the end of the 4-wk administration period beginning at 3 wk of age. B, Growth curves showing the naso-tail length during the administration of vehicle (●, n = 4) or 1 $\mu\text{g}/\text{kg} \cdot \text{min}$ CNP-22 (○, n = 4–5). *, $P < 0.05$. C, Soft x-ray examination of mice treated with vehicle (upper panel) or CNP-22 at a dose of 5 $\mu\text{g}/\text{kg} \cdot \text{min}$ (lower panel). D, Tibial lengths of ICR mice treated with vehicle (white bar) or 1 $\mu\text{g}/\text{kg} \cdot \text{min}$ CNP (black bar) for 4 wk. n = 4 (vehicle-treated group), and n = 3 (CNP-treated group). *, $P < 0.05$.

type mice. These results strongly indicate that CNP produced in the liver was able to affect the chondrocytes in the growth plate.

Effects of iv administration of CNP on endochondral bone growth of wild-type mice

Next we examined the effects of systemic CNP administration on bone growth in wild-type mice. The administration of synthetic CNP-22 to 3-wk-old mice via the jugular vein using a continuous infusion system equipped with a syringe pump resulted in a dose-dependent elevation of the plasma CNP-22 concentration. Plasma concentrations of CNP-22 measured using liquid chromatography-mass spectrometry (13) were 5.0 ± 0.3 and 29.3 ± 5.0 (mean \pm SD) ng/ml for infusion rates of 0.1 and 1.0 $\mu\text{g}/\text{kg}$ mouse body weight per minute, respectively, whereas the concentration was less than 0.2 ng/ml in vehicle-administered mice. Wild-type mice treated with CNP-22 at a dose of 1 $\mu\text{g}/\text{kg} \cdot \text{min}$ from the age of 3 wk were obviously longer than vehicle-treated mice after 1 wk iv CNP-22 treatment and were significantly elongated after the 4-wk administration period (Fig. 2, A and B). The naso-anal and naso-tail lengths of mice administered 1 $\mu\text{g}/\text{kg} \cdot \text{min}$ of CNP-22 were 12 and 10% longer, respectively, than those of vehicle-administered mice at the end of the 4-wk administration period (Fig. 2B). The body weights were not changed between the two groups (data not shown). Soft x-ray analysis revealed skeletal overgrowth in the CNP-22-administered mice (Fig. 3, C and D). Bone mineral density at the midshaft of the femur was not substantially different between the two groups [463 ± 30 and 527 ± 81 mg/ml³ (mean \pm SD) in groups administered vehicle and CNP-22, respectively; n = 4 for each group]. The thicknesses of the growth plates of the long bones

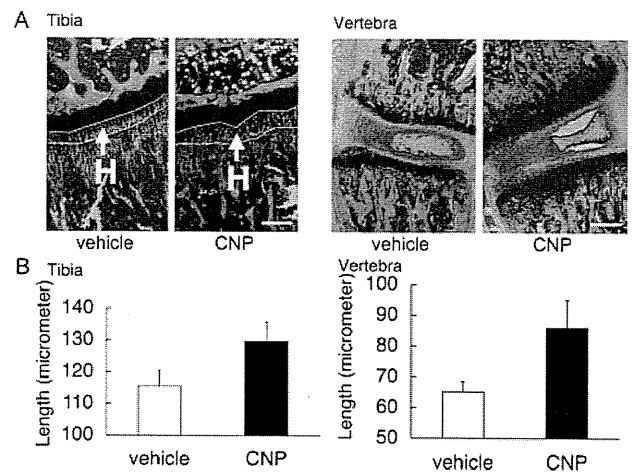


FIG. 4. Effects of systemic administration of CNP-22 on the growth plates of ICR mice. A, Histological pictures of the tibial (left two panels) and the vertebral (right two panels) growth plates of ICR mice administered vehicle (left panel in each group) or 1 $\mu\text{g}/\text{kg} \cdot \text{min}$ CNP (right panel in each group) for 4 wk and stained with safranin-O, hematoxylin, and eosin. Areas in the tibial growth plate between the yellow lines (denoted with an H) represent hypertrophic chondrocyte layers. Scale bar, 100 μm . B, Lengths of tibial (left panel) or vertebral (right panel) growth plates of ICR mice treated with vehicle (white bars) or 1 $\mu\text{g}/\text{kg} \cdot \text{min}$ CNP (black bars) for 4 wk, measured on histological pictures.

and vertebrae in the CNP-22-administered mice were greater than that in the vehicle-administered mice (Fig. 4A). The thicknesses of the tibial and vertebral growth plates in CNP-22-administered mice were 31 and 32% greater, respectively, than those in the vehicle-administered mice (Fig. 4B). Among the

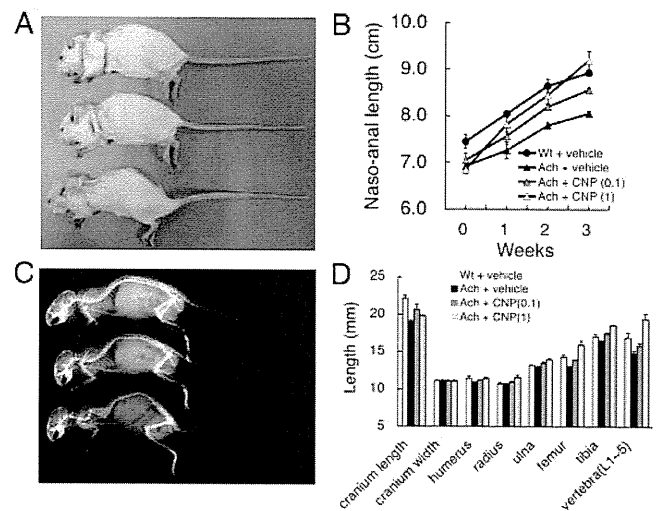


FIG. 5. Rescue of the Ach skeletal phenotype by CNP-22. Continuous iv administration was performed in 3-wk-old female wild-type (Wt) or Ach mice. A, Gross appearances of vehicle-treated Wt (upper panel), Ach (middle panel), or 1 $\mu\text{g}/\text{kg} \cdot \text{min}$ CNP-22 administered Ach (lower panel) mice at the end of the 4-wk administration period beginning at 3 wk of age. B, The dose-dependent effect of CNP-22 on the growth of Ach mice. Black circles, black triangles, gray triangles, and white triangles represent the naso-anal lengths of Wt mice treated with vehicle, Ach mice treated with vehicle, Ach mice treated with 0.1 $\mu\text{g}/\text{kg} \cdot \text{min}$ CNP-22, and Ach mice treated with 1 $\mu\text{g}/\text{kg} \cdot \text{min}$ CNP-22, respectively. The week after the commencement of treatment is shown on the x-axis. C, Soft x-ray analysis of Wt mice treated with vehicle, Ach mice treated with vehicle, and Ach mice treated with 1 $\mu\text{g}/\text{kg} \cdot \text{min}$ CNP-22 (from top to bottom) at the end of the 4-wk administration period. D, Bone lengths of Wt or Ach mice administered vehicle or CNP-22 for 4 wk. White bars, Wt mice treated with vehicle; black bars, Ach mice treated with vehicle; dark gray bars, Ach mice treated with 0.1 $\mu\text{g}/\text{kg} \cdot \text{min}$ CNP-22; light gray bars, Ach mice treated with 1 $\mu\text{g}/\text{kg} \cdot \text{min}$ CNP-22.

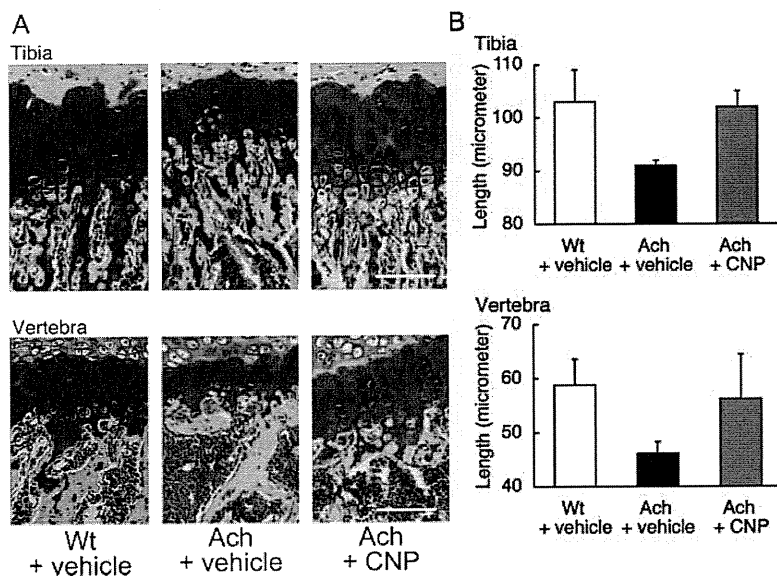


FIG. 6. Effects of systemic administration of CNP-22 on the growth plates of Ach mice. *A*, Histological pictures of the tibial (*upper panel*) and vertebral (*lower panel*) growth plates of mice treated with vehicle or CNP-22 for 4 wk. Samples were stained with safranin-O, hematoxylin, and eosin. From *left to right*, growth plate of a wild-type (Wt) mouse treated with vehicle, that of an Ach mouse treated with vehicle, and that of an Ach mouse treated with 1 $\mu\text{g}/\text{kg} \cdot \text{min}$ CNP-22. Scale bar, 50 μm . *B*, Lengths of tibial (*upper panel*) and vertebral (*lower panel*) growth plates of mice treated with vehicle or CNP-22 for 4 wk, measured on histological pictures. *White bars*, lengths of growth plates of Wt mice treated with vehicle; *black bars*, those of Ach mice treated with vehicle; *gray bars*, those of Ach mice treated with 1 $\mu\text{g}/\text{kg} \cdot \text{min}$ CNP.

growth plate layers, the hypertrophic chondrocyte layer was markedly thickened in response to CNP-22 (Fig. 4A).

We also investigated the effects of sc administration of CNP-22 using the same continuous infusion system; administration of similar doses, however, did not produce significant effects (data not shown).

Rescue of impaired bone growth of Ach mice by systemic administration of CNP

Based on the pilot study of CNP-22 in wild-type mice, CNP-22 was administered *iv* to 3-wk-old Ach mice. CNP-22 administration resulted in dose-dependent growth in Ach mice (Fig. 5, A and B). At the end of the 3-wk administration period, *iv* administration of CNP-22 at a dose of 0.1 $\mu\text{g}/\text{kg} \cdot \text{min}$ rescued 58% of the shortened naso-anal length phenotype of Ach mice, whereas a dose of 1 $\mu\text{g}/\text{kg} \cdot \text{min}$ resulted in mice that were longer than wild-type controls (Fig. 5, A and B). Soft x-ray analysis revealed promoted skeletal growth of Ach mice administered CNP at the dose of 1 $\mu\text{g}/\text{kg} \cdot \text{min}$ (Fig. 5C). Radius, ulna, femur, and tibia bones of Ach mice treated with 0.1 $\mu\text{g}/\text{kg} \cdot \text{min}$ CNP-22 were similar to those of vehicle-treated wild-type mice, whereas CNP-22 administration at a dose of 1 $\mu\text{g}/\text{kg} \cdot \text{min}$ resulted in longer bones than those from wild-type mice (Fig. 5D). The width of cranium, of which the growth is dependent on membranous ossification, was not changed between all groups (Fig. 5D). In histology, both the proliferative and hypertrophic chondrocyte layers in the tibial and vertebral growth plates were narrow in Ach mice, whereas they were comparable to those of wild-type mice after the administration of CNP at a dose of 1 $\mu\text{g}/\text{kg} \cdot \text{min}$ for 3 wk (Fig. 6). Hypertrophic chondrocytes were smaller in Ach mice than in wild-type mice, whereas after CNP-22

administration, they were similar in size to the hypertrophic chondrocytes of wild-type mice (Fig. 6A).

Discussion

The present study demonstrates that systemic administration of CNP is a novel therapeutic strategy for skeletal dysplasias including Ach. Previously, we exhibited that the CNP/GC-B system is a potent stimulatory system of endochondral bone growth in the growth plate; CNP and GC-B are expressed mainly in the pre-hypertrophic chondrocyte layer of the growth plate (8), and mice with targeted overexpression of CNP in the growth plate exhibit prominent skeletal overgrowth (7, 17), whereas mice depleted with CNP or GC-B exhibit short stature owing to their impaired bone growth (8, 9). We started the translational research of the growth-promoting effect of the CNP/GC-B system on bones into skeletal dysplasias, congenital disorders characterized by severe impairment of bone growth. In our previous report, we exhibited that targeted overexpression of CNP in the growth plate of Ach mice could rescue their impaired bone growth, demonstrating that CNP may be an effective treatment for this disorder (7).

In the present study, we have investigated whether or not systemic administration of CNP could be a drug therapy for skeletal dysplasias. We exhibited that blood-borne CNP from a CNP transgene specifically expressed in the liver or by continuous *iv* administration could recover the shortness and the impaired bone growth observed in Ach mice. We also verified the safety of circulating CNP whose plasma concentration affects bone growth; blood pressure, electrolytes, biochemical markers, and metabolic parameters were not significantly changed in SAP-CNP-Tg and wild-type mice. These results demonstrate that systemic administration of CNP is a possible drug therapy for Ach. Because current therapy for Ach generally is limited to distraction osteogenesis (4), an orthopedic procedure (5), and the benefit of distraction osteogenesis is limited, systemic administration of CNP can be a prominent therapeutic strategy for skeletal dysplasias including Ach.

As for the method of systemic administration of CNP, we also investigated the effects of sc administration of CNP-22 using the same continuous infusion system; administration of similar doses, however, did not produce significant effects. This finding could be a result of degradation of CNP-22 by neutral endopeptidase, which reportedly is abundantly expressed in sc tissues of mice (18). Future studies are necessary to evaluate neutral endopeptidase in sc tissues of humans other than mice.

The results showed that a higher plasma CNP-22 concentration was required to rescue the Ach phenotype in the mice with the infusion pump than in the Ach/SAP-CNP-Tg mice. In addition to CNP-22, CNP-53 is an endogenous form of CNP that has a longer biological half-life than CNP-22 (19). The degree of cross-reactivity of CNP-53 in the RIA for CNP is about 30% on a molar basis, indicating that the plasma of the transgenic mice

may contain CNP-53 and/or pro-CNP, a precursor of CNP that shows little cross-reactivity in the RIA. Further studies are necessary to elucidate the molecular forms of the CNP-LI proteins secreted from the liver in SAP-CNP-Tg mice. Another reason for the differences between the SAP-CNP-Tg mice and the infusion pump model may be that the increased levels of circulating CNP are present earlier during the development of the transgenic model, *i.e.* just after birth in Ach/SAP-CNP-Tg mice, compared with 3 wk of age for mice with the CNP infusion pump.

Safety analysis of the systemic administration of CNP-22 showed no change in systolic blood pressure. This is consistent with the result of our previous report demonstrating that systemically administered CNP in humans did not produce significant effects on hemodynamic parameters, including blood pressure (20). In addition, no adverse effects on bone mineral density or blood biochemistry, including electrolyte concentrations, were observed, indicating that chronic CNP treatment is safe. Nevertheless, safety issues with CNP need further study, because only short-term potential toxicity has been examined in the current study.

The clinical significance of CNP and its receptor, GC-B, in endochondral bone growth has been established in humans, because loss-of-function mutations in the human GC-B gene cause AMDM, a form of skeletal dysplasia (10, 11); the skeletal phenotypes similar to those of patients suffering from AMDM are also observed in GC-B knockout (9) and GC-B mutant (21, 22) mice. Among human skeletal dysplasias, AMDM is likely to be resistant to treatment with CNP. On the other hand, because spontaneous mutations in the mouse CNP gene (23, 24) are known to result in phenotypes identical to those observed in CNP knockout mice (8) and CNP mutant mice are rescued by targeted overexpression of CNP in their cartilage (25), patients with loss-of-function mutations in the CNP gene, which have not been reported to date, will likely be very sensitive to CNP administration. In addition, because administration of CNP could successfully stimulate the endochondral bone growth of wild-type mice, CNP would be potentially used for skeletal dysplasias other than achondroplasia or the putative form of skeletal dysplasia caused by loss-of-function mutations in the CNP gene. Recent progress in molecular genetics has identified mutations in various genes as the causes of skeletal dysplasias (1); therefore, in case we try to use CNP for the treatment of one form of skeletal dysplasia caused by mutations in a certain gene, we might better predict the therapeutic effects by investigating the molecular interactions between the gene product and CNP in endochondral ossification.

In conclusion, we have demonstrated the efficacy and safety of *iv* administration of CNP-22 for impaired endochondral bone growth in Ach mice. These results suggest that systemic administration of CNP or CNP analogs provides a novel therapeutic strategy for human skeletal dysplasias, including Ach.

Acknowledgments

We thank Dr. D.M. Ornitz (Department of Developmental Biology, Washington University Medical School) for Ach mice. We also thank Yoshihiro Ogawa for fruitful discussions and Shinji Yasuno for technical instruction.

Address all correspondence and requests for reprints to: Akihiro Yasoda, M.D., Ph.D., 54 Shogoin-Kawahara-cho, Sakyo-ku, Kyoto 606-8507, Japan. E-mail: yasoda@kuhp.kyoto-u.ac.jp.

This work was supported by a Grant-in-Aid for Scientific Research from the Ministry of Health, Labor, and Welfare of Japan and the Ministry of Education, Culture, Sports, Sciences, and Technology of Japan (19591075), a Grant-in-Aid from the Takeda Science Foundation, and a Novo Nordisk Growth and Development Study Award.

Disclosure Summary: T.F., E.K., M.M., N.K., Y.K. and H.A. have nothing to declare. A.Y. receives grant support (2008.12.1~2011.11.30) from Chugai Pharmaceutical Co., Ltd. H.K. and N.M. are employed by Chugai Pharmaceutical Co., Ltd. K.N. is an inventor of a related U.S. patent (US6743425) and patent applications in Japan (2003-113116 and 2003-104908), Canada (CA 2398030), and Brazil (BR200203172). N.M. is an inventor of patent application PCT/JJP2008/051472 (WO2008093762, applied only in Japan).

References

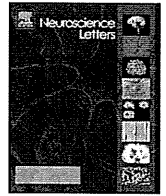
- Superti-Furga A, Bonafé L, Rimoin DL 2001 Molecular-pathogenetic classification of genetic disorders of the skeleton. *Am J Med Genet* 106:282–293
- Horton WA, Hall JG, Hecht JT 2007 Achondroplasia. *Lancet* 370:162–172
- Rousseau F, Bonaventure J, Legeai-Mallet L, Pelet A, Rozet JM, Maroteaux P, Le Merrer M, Munnich A 1994 Mutations in the gene encoding fibroblast growth factor receptor-3 in achondroplasia. *Nature* 371:252–254
- Cattaneo R, Villa A, Catagni M, Tentori L 1988 Limb lengthening in achondroplasia by Ilizarov's method. *Int Orthop* 12:173–179
- Horton WA, Hecht JT, Hood OJ, Marshall RN, Moore WV, Hollowell JG 1992 Growth hormone therapy in achondroplasia. *Am J Med Genet* 42:667–670
- Seino Y, Yamanaka Y, Shinohara M, Ikegami S, Koike M, Miyazawa M, Inoue M, Moriwake T, Tanaka H 2000 Growth hormone therapy in achondroplasia. *Horm Res* 53(Suppl 3):53–56
- Yasoda A, Komatsu Y, Chusho H, Miyazawa T, Ozasa A, Miura M, Kurihara T, Rogi T, Tanaka S, Suda M, Tamura N, Ogawa Y, Nakao K 2004 Overexpression of CNP in chondrocytes rescues achondroplasia through a MAPK-dependent pathway. *Nat Med* 10:80–86
- Chusho H, Tamura N, Ogawa Y, Yasoda A, Suda M, Miyazawa T, Nakamura K, Nakao K, Kurihara T, Komatsu Y, Itoh H, Tanaka K, Saito Y, Katsuki M, Nakao K 2001 Dwarfism and early death in mice lacking C-type natriuretic peptide. *Proc Natl Acad Sci USA* 98:4016–4021
- Tamura N, Doolittle LK, Hammer RE, Shelton JM, Richardson JA, Garbers DL 2004 Critical roles of the guanylyl cyclase B receptor in endochondral ossification and development of female reproductive organs. *Proc Natl Acad Sci USA* 101:17300–17305
- Bartels CF, Bükülmez H, Padayatti P, Rhee DK, van Ravenswaaij-Arts C, Pauli RM, Mundlos S, Chitayat D, Shih LY, Al-Gazali LI, Kant S, Cole T, Morton J, Cormier-Daire V, Faivre L, Lees M, Kirk J, Mortier GR, Leroy J, Zabel B, Kim CA, Crow Y, Braverman NE, van den Akker F, Warman ML 2004 Mutations in the transmembrane natriuretic peptide receptor NPR-B impair skeletal growth and cause acromesomelic dysplasia, type Maroteaux. *Am J Hum Genet* 75:27–34
- Hachiya R, Ohashi Y, Kamei Y, Suganami T, Mochizuki H, Mitsui N, Saitoh M, Sakuragi M, Nishimura G, Ohashi H, Hasegawa T, Ogawa Y 2007 Intact kinase homology domain of natriuretic peptide receptor-B is essential for skeletal development. *J Clin Endocrinol Metab* 92:4009–4014
- Naski MC, Colvin JS, Coffin JD, Ornitz DM 1998 Repression of hedgehog signaling and BMP4 expression in growth plate cartilage by fibroblast growth factor receptor 3. *Development* 125:4977–4988
- Murao N, Ishigai M, Yasuno H, Shimonaka Y, Aso Y 2007 Simple and sensitive quantification of bioactive peptides in biological matrices using liquid chromatography/selected reaction monitoring mass spectrometry coupled with trichloroacetic acid clean-up. *Rapid Commun Mass Spectrom* 21:4033–4038
- Komatsu Y, Nakao K, Suga S, Ogawa Y, Mukoyama M, Arai H, Shirakami G, Hosoda K, Nakagawa O, Hama N, Kishimoto I, Imura H 1991 C-type natriuretic peptide (CNP) in rats and humans. *Endocrinology* 129:1104–1106
- Suda M, Ogawa Y, Tanaka K, Tamura N, Yasoda A, Takigawa T, Uehira M, Nishimoto H, Itoh H, Saito Y, Shiota K, Nakao K 1998 Skeletal overgrowth in transgenic mice that overexpress brain natriuretic peptide. *Proc Natl Acad Sci USA* 95:2337–2342
- Ogawa Y, Itoh H, Tamura N, Suga S, Yoshimasa T, Uehira M, Matsuda S, Shiono

- S, Nishimoto H, Nakao K 1994 Molecular cloning of the complementary DNA and gene that encode mouse brain natriuretic peptide and generation of transgenic mice that overexpress the brain natriuretic peptide gene. *J Clin Invest* 93:1911–1921
17. Miyazawa T, Ogawa Y, Chusho H, Yasoda A, Tamura N, Komatsu Y, Pfeifer A, Hofmann F, Nakao K 2002 Cyclic GMP-dependent protein kinase II plays a critical role in C-type natriuretic peptide-mediated endochondral ossification. *Endocrinology* 143:3604–3610
 18. Sales N, Dutriez I, Maziere B, Ottaviani M, Roques BP 1991 Neutral endopeptidase 24.11 in rat peripheral tissues: comparative localization by 'ex vivo' and 'in vitro' autoradiography. *Regul Pept* 33:209–222
 19. Minamino N, Kangawa K, Matsuo H 1990 N-terminally extended form of C-type natriuretic peptide (CNP-53) identified in porcine brain. *Biochem Biophys Res Commun* 170:973–979
 20. Igaki T, Itoh H, Suga SI, Hama N, Ogawa Y, Komatsu Y, Yamashita J, Doi K, Chun TH, Nakao K 1998 Effects of intravenously administered C-type natriuretic peptide in humans: comparison with atrial natriuretic peptide. *Hypertens Res* 21:7–13
 21. Tsuji T, Kunieda T 2005 A loss-of-function mutation in natriuretic peptide receptor 2 (Npr2) gene is responsible for disproportionate dwarfism in *cn/cn* mouse. *J Biol Chem* 280:14288–14292
 22. Sogawa C, Tsuji T, Shinkai Y, Katayama K, Kunieda T 2007 Short-limbed dwarfism: *slw* is a new allele of *Npr2* causing chondrodysplasia. *J Hered* 98:575–580
 23. Jiao Y, Yan J, Jiao F, Yang H, Donahue LR, Li X, Roe BA, Stuart J, Gu W 2007 A single nucleotide mutation in *Nppc* is associated with a long bone abnormality in *lbab* mice. *BMC Genet* 8:16
 24. Yoder AR, Kruse AC, Earhart CA, Ohlendorf DH, Potter LR 2008 Reduced ability of C-type natriuretic peptide (CNP) to activate natriuretic peptide receptor B (NPR-B) causes dwarfism in *lbab* $-/-$ mice. *Peptides* 29:1575–1581
 25. Tsuji T, Kondo E, Yasoda A, Inamoto M, Kiyosu C, Nakao K, Kunieda T 2008 Hypomorphic mutation in mouse *Nppc* gene causes retarded bone growth due to impaired endochondral ossification. *Biochem Biophys Res Commun* 376:186–190



Contents lists available at ScienceDirect

Neuroscience Letters

journal homepage: www.elsevier.com/locate/neulet

Orexins increase mRNA expressions of neurotrophin-3 in rat primary cortical neuron cultures

Nobuko Yamada^{a,b,*}, Goro Katsuura^{a,d}, Ichiro Tatsuno^b, Shigenori Kawahara^c,
Ken Ebihara^a, Yasushi Saito^b, Kazuwa Nakao^a

^a Department of Medicine and Clinical Science, Kyoto University Graduate School of Medicine, 54 Kawahara-cho, Shogoin, Sakyo-ku, Kyoto 606-8507, Japan

^b Department of Clinical Cell Biology, Chiba University Graduate School of Medicine, 1-8-1 Inohana, Chuo-ku, Chiba 260-8670, Japan

^c Graduate School of Science and Engineering, University of Toyama, 3190 Gofuku, Toyama 930-8555, Japan

^d Pharmaceutical Research & Development Division, Strategic Development Department, Shionogi & Co., Ltd., 12-4 Sagisu 5-chome, Fukushima-ku, Osaka 553-0002, Japan

ARTICLE INFO

Article history:

Received 1 September 2008

Received in revised form 28 October 2008

Accepted 11 November 2008

Keywords:

Orexin

Melanin-concentrating hormone

Neurotrophin-3

Brain-derived neurotrophic factor

Rat primary cortical neuron cultures

Real-time PCR

ABSTRACT

Orexins and melanin-concentrating hormone (MCH) as orexigenic neuropeptides are present in the lateral hypothalamus, and their receptors are distributed in the cerebral cortex and hippocampus. In the present study, the regulatory effects of orexin-A, orexin-B and MCH on neurotrophin-3 (NT-3) and brain-derived neurotrophic factor (BDNF) expressions were examined in primary cortical neuron cultures using quantitative real-time PCR. Both orexin-A and orexin-B on 6-day exposure significantly increased the NT-3 mRNA at concentrations of 0.01, 0.1 and 1 μ M. Orexin-A and B at 1 μ M led to an increase of twofold or more over the control. However, no such NT-s mRNA increase occurred with exposure to MCH at the same concentrations as orexins. The mRNA expression of BDNF was significantly increased only by orexin-B at 1 μ M. These findings suggest that orexins, but not MCH, may be an inducer of NT-3 in the cerebral cortex.

© 2008 Elsevier Ireland Ltd. All rights reserved.

Orexins (orexin-A, orexin-B) and melanin-concentrating hormone (MCH) are orexigenic neuropeptides predominantly present in the lateral hypothalamus [23]. The orexin receptors (OX1R, OX2R) and MCH receptors (MCHR1) are distributed at high concentrations in the cerebral cortex and hippocampus [12]. These areas are postulated to play an important role in regulating the higher functions of the central nervous system, such as learning and memory, based on neuronal plasticity. In this regard, orexin has been reported to play a critical role in neuronal plasticity relevant to addiction in the ventral tegmental area and in long-term potentiation of synaptic transmission in the hippocampus [4,24]. MCH was also found to increase hippocampal synaptic transmission via increased synaptic efficacy [29]. Recently, we demonstrated that in rat primary cortical neuron cultures orexins and MCH decreased the expression of subunits of the NMDA (*N*-methyl-*D*-aspartate) receptor and the AMPA (α -amino-3-hydroxy-5-methyl-4-isoxazole propionic acid) receptor [31]. These findings suggest that orexin and MCH may regulate the higher functions, such as cognition and emotion, of the

central nervous system as well as energy regulation. Moreover, neurotrophic factors also play an important role in regulating neuronal plasticity in the brain. The neurotrophin family includes brain-derived neurotrophic factor (BDNF), nerve growth factor (NGF), neurotrophin-3 (NT-3), neurotrophin-4 (NT-4) and neurotrophin-5 (NT-5) [15]. They exert their biological functions via each of the specific tyrosine kinase receptors (Trk) [2,5]. In the mature nervous system, neurotrophic factors, especially BDNF and NT-3, are demonstrated to be widely distributed in the brain, where they regulate the activity-dependent synaptic plasticity which is involved in the learning and memory regulation [22,27].

In this study, to explore the functions of orexin and MCH in the cerebral cortex, we examined the effects of chronic application of orexin and MCH on NT-3 and BDNF mRNA expressions using primary cortical neuron cultures.

For preparing rat cultured primary cortical neurons timed pregnant Sprague–Dawley rats were obtained from Japan SLC, Inc. (Japan) on gestational day 18. The animals were anesthetized with pentobarbital sodium (50 mg/kg, ip; Abbott, Abbott Park, IL, USA) and sacrificed by cervical dislocation. The fetuses were delivered and decapitated. In each experiment, fetuses were extracted from four maternal rats. All experiments were performed in accordance with the guideline established by the Institutional Animal Investigation Committee at Kyoto University (Med Kyo 06514), Chiba

* Corresponding author at: Department of Medicine and Clinical Science, Kyoto University Graduate School of Medicine, 54 Kawahara-cho, Shogoin, Sakyo-ku, Kyoto 606-8507, Japan. Tel.: +81 757513171; fax: +81 757719452.

E-mail address: nobukito@kuhp.kyoto-u.ac.jp (N. Yamada).